



# Analysis of crosstalk in high speed and high frequency printed circuit board

Avali Ghosh , Sisir Kumar Das and Annapurna Das

Department of Electronics and Communication Engineering, Maulana Abul Kalam Azad University of Technology, Kolkata, India

## ABSTRACT

Numerical analysis of crosstalk between two traces in a printed circuit board is presented using the method of moments (MoM). In the high-frequency range, the attenuation constant is neglected in the theory for its very small values. The width of the trace is accurately determined for the trace impedance of 50 ohm from the charge distribution on the traces without using an approximated empirical formula. Line capacitances are determined from the total charge on the conductors and the line potentials. The coupling capacitance and inductance are determined from in-phase and out-of-phase excitations between the traces. Crosstalk interference is calculated from these coupling parameters. Results of crosstalk obtained from the above technique are verified by comparing with those obtained from four other methods: (1) Ansoft HFSS software tool, (2) even mode and odd mode analysis, (3) empirical formulae of parasitic elements, and (4) measurements using a vector network analyser. All the results agreed well. The results obtained by using the method of moment technique are more stable, reliable, and accurate among all the described different methods. This paper shows that the analytical method using MoM is a useful tool for predicting crosstalk interference in PCB without using expensive simulation software.

## ARTICLE HISTORY

Received 5 May 2020  
Accepted 4 October 2020

## KEYWORDS

Crosstalk; electromagnetic compatibility; electromagnetic interference; method of moments; mutual coupling

## 1. Introduction

In the design of high-speed and high frequency printed circuit board (PCB) several electromagnetic compatibility (EMC) and signal integrity (SI) problems arise due to distributed characteristics of the traces. The designers find solutions to these problems using costly software tools and engineering judgement. One of the most important issues is the undesired signal coupling or crosstalk interference from a source trace to adjacent traces that takes place through the stray capacitance and mutual inductance between two adjacent traces. Therefore, determinations of stray capacitance and mutual inductance between the traces are very important for crosstalk calculation. Most of the analytical methods of solution for finding these parameters require a specific choice of electric charge distribution on the traces. These methods encounter mathematical complexity

**CONTACT** Avali Ghosh  [avalighosh@gmail.com](mailto:avalighosh@gmail.com);  [avali.banerjee@gnit.ac.in](mailto:avali.banerjee@gnit.ac.in) Guru Nanak Institute of Technology, 157/F, Nilgunj Road, Panihati, Sodepur, Kolkata 700114, India

Scopus Author ID: 55490524900

© 2021 Informa UK Limited, trading as Taylor & Francis Group

## Green biosynthesis of silver nanoparticles using *Dregea volubilis* flowers: Characterization and evaluation of antioxidant, antidiabetic and antibacterial activity

Bhaskar Das<sup>a</sup>, Arnab De<sup>a</sup>, Soumik Podder<sup>b</sup>, Shilpa Das<sup>a</sup>, Chandan Kumar Ghosh<sup>b</sup>, and Amalesh Samanta<sup>a</sup>

<sup>a</sup>Division of Microbiology and Biotechnology, Department of Pharmaceutical Technology, Jadavpur University, Kolkata, India; <sup>b</sup>School of Materials Science and Nanotechnology, Jadavpur University, Kolkata, India

### ABSTRACT

The present work was conducted to biofabricate silver nanoparticles (AgNPs) in single step employing aqueous extract of *Dregea volubilis* flowers and to investigate its antioxidant, antidiabetic and antibacterial activities. The AgNPs were characterized by UV-Visible spectroscopy, X-ray diffraction (XRD), Fourier transform infrared spectroscopy (FTIR), field emission scanning electron microscopy (FESEM), energy-dispersive X-ray (EDX) spectrometry, high resolution transmission electron microscopy (HRTEM) and zeta potential study. The biofabricated AgNPs showed potential antioxidant activity for scavenging DPPH radical (IC<sub>50</sub>, 40.45 ± 5.06 µg/mL), ABTS radical (IC<sub>50</sub>, 78.49 ± 1.41 µg/mL), total antioxidant capacity (148.83 ± 2.99 mg GAE/g) along with remarkable inhibitory effects on α-amylase (IC<sub>50</sub>, 10.62 ± 0.22 µg/mL) and α-glucosidase (IC<sub>50</sub>, 6.49 ± 0.03 µg/mL). The AgNPs showed notable antibacterial activity in terms of zone of inhibition (in mm) against *Pseudomonas aeruginosa* (10.67 ± 0.44), *Escherichia coli* (9.33 ± 0.44), *Bacillus subtilis* (14.67 ± 0.60) and *Staphylococcus aureus* (15.67 ± 0.60).

### ARTICLE HISTORY

Received 16 May 2020  
Accepted 2 August 2020

### KEYWORDS

Silver nanoparticles; *Dregea volubilis* flower; antioxidant activity; α-Glucosidase inhibitory activity; α-Amylase inhibitory activity

### Introduction

Nanotechnology is a branch of science with interdisciplinary approach which has received considerable attention in recent years to researchers from different fields like life sciences, material sciences, biomedical engineering, chemistry, and physics.<sup>[1]</sup> The synthesis of nanoscale materials and structures of different shapes and sizes has received increasing recognition due to their versatile uses in several technological and medical applications.<sup>[2]</sup> Nanoparticles usually ranging from 1 to 100 nanometer (nm) are of great interest due to their extremely diminutive size and large surface to volume ratio with contrasting physicochemical properties compared to their bulk materials of an identical chemical composition.<sup>[3]</sup> Silver is a well-recognized metal and its use can be traced back to times even before Neolithic revolution whereas the medicinal use of silver was recorded during 8th century.<sup>[4]</sup> Among the noble metal nanoparticles silver nanoparticles (AgNPs) has gained more scientific attention due to its extraordinary features of exceptional magnetic, optical and electronic properties for which AgNPs has gained extensive applications in various fields of science and technology such as catalysis, optoelectronics, photonics, pharmaceuticals, biomedical, antimicrobial products, electronics, sensing, therapeutics, and so on.<sup>[5]</sup> Nanoparticles synthesis involves venomous chemicals and elevated energy physical methods which produce vast number of unsafe byproducts resulting

in contamination of the environment.<sup>[6]</sup> There is a need to develop green nanotechnology which is clean, nontoxic, environmentally friendly and cost effective in contrast with chemical and physical methods employed for synthesis of nanoparticles.<sup>[7]</sup> The environmentally benign biogenic synthesis methods using nontoxic materials such as microorganisms, whole plants, different parts of plants, plant extracts and marine algae from salts of the corresponding metals as green synthesis of metal nanoparticles are aimed at protecting the health of planet by preventing pollution, and moving toward sustainability. The biogenic synthesis of metal nanoparticles using plant extracts could be advantageous over other environmentally benign biological routes of synthesis by quashing the laborious process of maintaining cell cultures. Plants contain thousands of biologically active compounds such as alkaloids, tannins, phenolics, saponins, terpenoids, polysaccharides, proteins and vitamins which can act both as reducing agents and stabilizing agents in the synthesis of metal nanoparticles.<sup>[7]</sup> Phytochemicals with functional groups such as carbonyl, hydroxyl, and amine have the ability of reducing metal ions and capping the newly formed metal nanoparticles during their growth processes.<sup>[8]</sup> Multidrug resistant bacterial strains arising due to mutation, pollution and changing environmental conditions are a major problem in human life and metal nanoparticles especially AgNPs occupy an important place among such nanoparticles as antimicrobial agents to curb such a

# RECENT ADVANCES OF FACE RECOGNITION IN TRANSFORM DOMAIN

Suparna Biswas<sup>1</sup>, Sayan Roy Chowdhuri<sup>2</sup>, Palasri Dhar<sup>3</sup>, Suparna Karmakar<sup>4</sup>

<sup>1,2,3</sup> Department of Electronics and Communication Engineering

<sup>4</sup> Department of Information Technology, Guru Nanak Institute of Technology, Panihati, Sodepur, India, 700114.

Emails: <sup>1</sup>suparna.biswas@gnit.ac.in, <sup>2</sup>sayan.roychaudhuri@gnit.ac.in, <sup>3</sup>palasri.dhar@gnit.ac.in, <sup>4</sup>suparna.karmakar@gnit.ac.in

Received: 14 April 2020 Revised and Accepted: 8 August 2020

**ABSTRACT.** This paper provides a review on recent advances of face recognition techniques on two dimensional images. At first we have presented an overview of face recognition and its application. Then an attempt is made to review wide range of methods in frequency domain used for face recognition such as Discrete Fourier Transform (DFT), Discrete Cosine Transform (DCT), Discrete Wavelet Transform and Contourlet Transform (CT). This review at first described the different transform domain for 2D image and then investigates the recognition accuracy of different face recognition methods on different databases in the DFT, DCT, DWT and CT domain. Description, benefits and limitations of different transform domain based face recognition approaches are also discussed in this literature.

**KEYWORDS:** Discrete Fourier Transform (DFT), Discrete Cosine Transform (DCT), Discrete Wavelet Transform (DWT), Contourlet Transform (CT).

## 1. INTRODUCTION

Face recognition (FR) method is a widely used technology for identification or verification of a person from digital image. The objective of this technique is to identify a person or individuals from face images. Among different biometric based approaches (such as face, fingerprints, signature, iris recognition), FR offer various merits over other biometric methods.

There are different applications of FR such as, **Access and Security:** Instead of using password or passcode at present mobile phones and consumer electronics are accessed via facial features.

In future FR can be applied to get access into their houses, vehicles and other secure locations.

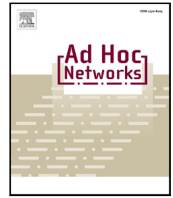
Different organization or companies which handles sensitive data, needs strict control on who enters their facilities. Advanced FR can be applied in these situations for security purpose.

**Criminal Identification:** Criminal identification is another important application of FR. At present US FBI is trying to catch or track suspect by applying machine learning based FR from

their driver's licenses (stored database). **Advertisement:** Traditionally Face technology has been associated with the security sector but now a day it has an active application in healthcare and advertisement.

FR is a demanding task in the field of image analysis processing. Different researchers are solving different challenges like pose variations, differences of illumination, variations of expressions and occlusions etc. Efficient FR method associated with proper preprocessing technique of images can reduce the effect of noise, pose variations, occlusions and illumination

*Keywords: A survey of FR methods mainly depends on two important terms: Feature extraction*



# On energy efficient secure routing in multi-hop underlay D2D communications for IoT applications

Surajit Basak<sup>a</sup>, Tamaghna Acharya<sup>b,\*</sup>

<sup>a</sup> Department of Electronics & Communication Engineering, Guru Nanak Institute of Technology, Kolkata 700114, India

<sup>b</sup> Department of Electronics & Telecommunication Engineering, Indian Institute of Engineering Science and Technology, Shibpur 711103, India

## ARTICLE INFO

### Keywords:

Spectrum sharing  
Multi-hop device-to-device communication  
Physical layer security  
Secrecy energy efficiency

## ABSTRACT

In this paper, a physical layer security based secure routing problem in a multi-hop cognitive radio enabled device-to-device (CRD2D) communication, under the threat of multiple randomly distributed eavesdroppers (EVEs), is studied. Delivery of confidential packets between a given legitimate D2D transmitter–receiver pair is targeted with the aid of multiple intermediate legitimate D2D nodes that share spectrum of a predefined licensed/primary user for their transmissions as unlicensed/secondary users and operate on the principle of randomized-and-forward relaying. In view of the energy limitations of the D2D nodes engaged in IoT applications, the secure routing problem aims to maximize the secrecy energy efficiency (SEE) under the constraints of – (i) minimum secrecy rate (ii) minimum signal-to-interference plus noise ratio at any D2D receiver (iii) maximum primary user outage loss in presence of the D2D transmission (iv) maximum retransmission attempts by any D2D nodes. Based on our analysis, an optimal routing algorithm is proposed. Simulation results illustrate the dependence of SEE on various critical system parameters. Further, complexity analysis and implementation issues are also presented for the proposed routing algorithm.

## 1. Introduction

Among the different types of communication modes being investigated for interconnecting Internet of Things (IoT) devices, device-to-device (D2D) communication is a prominent networking paradigm in 5G that allows two nearby devices to exchange data with each other without traversing any base station or access points [1,2]. Fortunately, with the recent advancements of cognitive radio (CR) technology, nodes using D2D communications are encouraged to share the spectrum of licensed users (also known as primary users (PUs)) without causing adverse impact on their communications. CR based device-to-device (CRD2D) networks, are highly attractive for next generation networks for enhanced spectrum efficiency, reduced energy consumption [3] and improved end-to-end (e2e) delay performance [4].

Despite appreciable potential of D2D communications, the direct connections between devices are vulnerable to various security and privacy threats because of the broadcasting nature of wireless transmission. Thus, security issue has been imperative for confidential data transmission (such as financial transactions, sensitive voice, video, and message transmission) between D2D users. With the gradual weakening of the validity of the assumption on the limitation of the computational capability of the eavesdropper (EVE) and power limited, delay sensitive and processing restricted features of CRD2D communication,

traditional cryptographic approaches alone would find it difficult to deliver a highly secure solution for D2D communication. To this end, physical layer security (PLS), which exploits the physical characteristics (e.g. multipath fading, propagation delay, etc.) of wireless channel to increase security, has been motivating researchers to design secure communication protocols in presence of the unauthorized EVE [5–9].

Typical performance metrics used to evaluate a PLS based solution are secrecy rate, secrecy outage probability (SOP), secrecy throughput and secrecy energy efficiency (SEE). The secrecy rate is popularly defined as the difference of data rate between the legitimate channel and the EVE channel [7]. In absence of the perfect knowledge on the EVE's instantaneous channel state information (CSI), secrecy rate is replaced by SOP. The SOP is defined as the probability that the secrecy rate falls below some threshold confidential information rate [10]. However, maximizing only secrecy rate or minimizing only SOP demands enhanced transmit power consumption that can shorten the limited battery lifetime of the D2D nodes and it is especially true when D2D is used in IoT applications. The SEE for a point-to-point D2D communication is defined as the ratio of secrecy throughput attained at a given link to the power consumption of the transmitter following [8].

Moreover, the additional burden of relaying, in terms of power consumption, on the D2D nodes that are coupled with any multi-hop

\* Corresponding author.

E-mail addresses: [surajit.basak2007@gmail.com](mailto:surajit.basak2007@gmail.com) (S. Basak), [t\\_acharya@telecom.iiests.ac.in](mailto:t_acharya@telecom.iiests.ac.in) (T. Acharya).

## Highly Sensitive Formaldehyde Based on Hierarchical ZnO Nanostructure to Defeat Sick Building Syndrome

<sup>1</sup>Paramita Chowdhury, <sup>2,\*</sup>Sunipa Roy, <sup>2</sup>Nabaneeta Banerjee,  
<sup>3</sup>Swapan Das and <sup>4</sup>Utpal Biswas

<sup>1</sup> Department of Electronics & Communication Engineering, Netaji Subhash Engineering College,  
Kolkata-700152, India

<sup>2</sup> Department of Electronics & Communication Engineering, Guru Nanak Institute of Technology,  
Kolkata-700114, India

<sup>3</sup> IC Design and Fabrication Center, Department of Electronics and Telecommunication Engineering,  
Jadavpur University, Kolkata 700032, India

<sup>4</sup> Department of Computer Science & Engineering, University of Kalyani, Nadia-741235, India  
Tel.: 9830751850

E-mail: sunipa\_4@yahoo.co.in

*Received: 4 February 2021 /Accepted: 17 March 2021 /Published: 31 March 2021*

---

**Abstract:** Zinc oxide (ZnO) hierarchical Nanofoam structure on ZnO nanofibers grown SiO<sub>2</sub> coated p-Si substrate were successfully constructed under chemical deposition technique by forming a homogeneous solution of Sodium Zincate (Na<sub>2</sub>ZnO<sub>2</sub>) in Teflon-lined Autoclave at 120 °C. The seed layer of hierarchical ZnO nanostructure was formed by Sol-gel technique followed by CBD (Chemical bath deposition) technique to grow ZnO nanofibers. The surface morphology and crystallinity of the thin film was characterized by scanning electron microscope (SEM) and X-ray diffraction (XRD) and controlled by adjusting the pH of the reaction solution. The hierarchical ZnO Nanostructure based Formaldehyde (HCHO) Sensor was tested in the resistive mode at dynamic range of 190 ppm to 2020 ppm formaldehyde vapour to defeat sick building syndrome. It was found to offer high response magnitude 94.8 % at 2020 ppm at very low optimum operating temperature 100 °C with fast response time (20 s). Finally, the possible mechanism of decomposition of formaldehyde sensor has been discussed with detailed explanation of higher response magnitude on exposure of formaldehyde vapour with energy band diagram.

**Keywords:** ZnO hierarchical nanostructure, ZnO nanofibers, Teflon-lined Autoclave, Formaldehyde sensor, Sensing mechanism, Energy band diagram.

---

### 1. Introduction

Hierarchical nanostructure has ushered with immense possibilities as there are much scope to explore the opportunities with the use of it [1-3]. By controlling their physical, chemical properties with modifying their shapes and morphology the

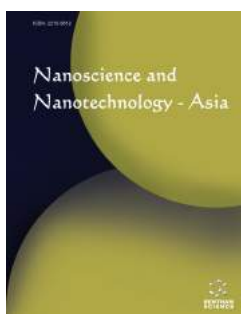
effectiveness of this hierarchical nanostructure can be varied in a broad way. There are many reports till date with 3-D nanostructures [2-4]. But lower surface area with limited gas interaction facets, these types of nanostructures cannot compete as a next generation gas sensor. Researchers are looking for some new developments as next generation gas sensors are



(/)

Search for...

Q Search

Search in:  All  Article  Chapter  Book[Purchase PDF](#)

Research Article

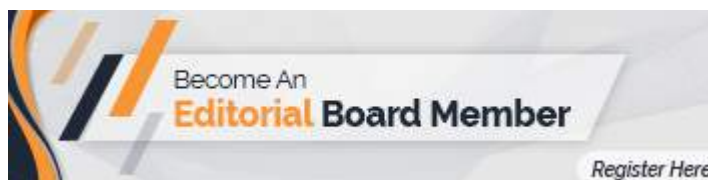
## Facile Synthesis of ZnO Nanofoam on ZnO Nanowire for Hydrogen Gas Detection

**Author(s):** Paromita Chowdhury, Sunipa Roy\*, Nabaneeta Banerjee, Kuheli Dutta, Utpal Gangopadhaya, Utpal Biswas

**Journal Name:** Nanoscience & Nanotechnology-Asia

**Volume 10 , Issue 1 , 2020**

**DOI :** 10.2174/2210681208666180927103948 (<https://doi.org/10.2174/2210681208666180927103948>)

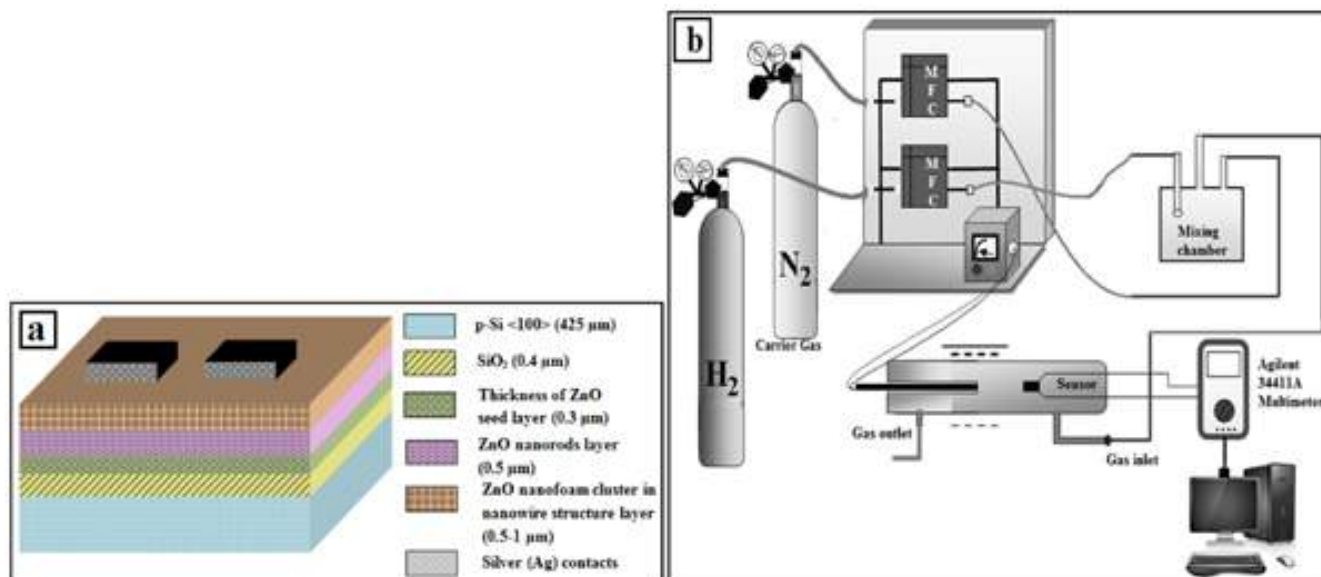
[🏠 Journal Home \(/node/694\)](#)

(<https://www.eurekaselect.com/node/694/nanoscience-nanotechnology-asia/become-ebm-form/eabm>)



(<https://www.eurekaselect.com/node/694/nanoscience-nanotechnology-asia/become-ebm-form/reviewer>)

### Graphical Abstract:



## Abstract:

**Background:** ZnO nanofoam cluster was deposited on ZnO nanowires using  $\text{SiO}_2/\text{Si}$  substrate. Nanocrystalline ZnO nanofoam cluster was grown on Chemical Bath Deposition (CBD) grown ZnO nanowires by consecutive immersion (50 times) of the sample into Sodium Zincate ( $\text{Na}_2\text{ZnO}_2$ ) bath (0.125M) kept at room temperature and into the de-ionized (DI) water maintained at 80°C.

**Methods:** Sodium Zincate was prepared by reacting Zinc Sulphate ( $\text{ZnSO}_4$ ) and excess Sodium Hydroxide ( $\text{NaOH}$ ) in aqueous solution. By simple Chemical Bath Deposition (CBD) technique ZnO nanowires of length of 1-1.5  $\mu\text{m}$  with diameter 2-3 nm were deposited on  $\text{SiO}_2$  coated  $\langle 100 \rangle$  p-Si substrate. The ZnO nanofoam cluster area was found to be  $\sim(0.5 \times 0.5) \mu\text{m}^2$ . After structural and morphological characterizations by FESEM, EDX and AFM, the sensor was tested for three different  $\text{H}_2$  concentrations (0.1, 0.5 and 1%) taking  $\text{N}_2$  as carrier gas at four different operating temperatures (50°C, 75°C, 100°C and 125°C).

**Results:** The sensor offered  $\sim 98\%$  response magnitude at very low operating temperature 100°C at 1000 ppm  $\text{H}_2$  gas with very fast response time (16 sec) and recovery time (52 sec). The unique structure of nanofoam covers multidimensional area having more molecular surface interactions thus permitting better response in gas sensing. The I-V characteristics was studied to indicate ohmic nature of the silver contacts for four operating temperatures with 1% hydrogen in  $\text{N}_2$  and it was also observed that amplitude of current is higher with the presence of  $\text{H}_2$ .

**Conclusion:** Finally the stability study of the  $\text{H}_2$  sensor was also done in presence of carrier gas ( $\text{N}_2$ ) over a span of 24 hours (6 hr daily).

**Keywords:** ZnO nanofoam, ZnO nanowire, chemical bath deposition,  $\text{H}_2$  sensing, I-V characteristics, stability.

References: [➤](#)

Mark Item

Purchase PDF

Rights & Permissions

Print

Export

Cite as

Other

## Article Details

VOLUME: 10

ISSUE: 1

Year: 2020

**Published on: 23 January, 2020**

Page: [86 - 92]

Pages: 7

DOI: 10.2174/2210681208666180927103948

(<https://doi.org/10.2174/2210681208666180927103948>)

Price: \$25

### Article Metrics

PDF: 13

HTML: 3

### Most Downloaded Article(s)

Magnetic Fe<sub>3</sub>O<sub>4</sub> Nanoparticles: Synthesis and Application in Water Treatment

(<https://www.eurekaselect.com/node/95785/?tracking-code=4>)

Nanoscience & Nanotechnology-Asia

Optimization of Itraconazole Solid Lipid Nanoparticles for Topical Delivery

(<https://www.eurekaselect.com/node/167268/?tracking-code=4>)

Nanoscience & Nanotechnology-Asia

Frequency Encoded All Optical Tri-state Logic Gates NOT and NAND Using Semiconductor Optical Amplifier Based Interferometric Switches

(<https://www.eurekaselect.com/node/172855/?tracking-code=4>)

Nanoscience & Nanotechnology-Asia

Optimization of Solid Lipid Nanoparticles of Ezetimibe in Combination with Simvastatin Using Quality by Design (QbD)

(<https://www.eurekaselect.com/node/170057/?tracking-code=4>)

Nanoscience & Nanotechnology-Asia

Developmental Studies of Curcumin NLCs as Safe Alternative in Management of Infectious Childhood Dermatitis

(<https://www.eurekaselect.com/node/168592/?tracking-code=4>)

Nanoscience & Nanotechnology-Asia

Source/Drain Stressor Design for Advanced Devices at 7 nm Technology Node

(<https://www.eurekaselect.com/node/174215/?tracking-code=4>)

Nanoscience & Nanotechnology-Asia

A New Tool for Simulation of Single Electron Transistor based Microprocessor Using Vector File

(<https://www.eurekaselect.com/node/175630/?tracking-code=4>)

Nanoscience & Nanotechnology-Asia

Enhancement of Separated Ultra Pure n-paraffin as Phase Change Materials (PCM) by W-Fe Bimetallic Oxides

(<https://www.eurekaselect.com/node/174161/?tracking-code=4>)

Nanoscience & Nanotechnology-Asia

Combine Drug Delivery of Thymoquinone-Doxorubicin by Cockle Shell-derived pH-sensitive Aragonite CaCO<sub>3</sub> Nanoparticles

(<https://www.eurekaselect.com/node/172037/?tracking-code=4>)

Nanoscience & Nanotechnology-Asia

Terahertz Radiators Based on Si~3C-SiC MQW IMPATT Diodes

(<https://www.eurekaselect.com/node/174163/?tracking-code=4>)

Nanoscience & Nanotechnology-Asia

(/terms/termandcondition.html?1)

© 2020 Bentham Science Publishers (<https://www.eurekaselect.com/136826/page/terms-and-conditions>) | Privacy Policy (<https://www.eurekaselect.com/180856/page/bentham-science-privacy-notice-may-2018>)



(<https://www.projectcounter.org/counter-user/bentham-science/>)

# Efficient Room Temperature Hydrogen Gas Sensor using ZnO Nanoparticles-Reduced Graphene Oxide Nanohybrid

Swapan Das, Sunipa Roy, *Senior Member, IEEE*, Tara Shankar Bhattacharya and Chandan Kumar Sarkar, *Senior Member, IEEE*

**Abstract**—In this work, a highly sensitive room-temperature hydrogen gas-sensor based on reduced graphene oxide (rGO) and zinc oxide nanoparticles (ZnO NPs) nanohybrid structure is reported. ZnO NPs were grown by chemical deposition method while the rGO layer was produced by the electrochemical exfoliation using tetramethyle ammonium hydroxide (TMAH) as organic solvent and then drop-casted on the ZnO NPs layer. The detailed morphological (FESEM) and structural (Raman and XPS) analysis were carried out to compare different properties of pristine ZnO NPs and rGO-ZnO NPs hybrid structure. The rGO-ZnO NPs nanohybrid sensor with a Pd-Ag (70%) catalytic contact was tested for five different hydrogen concentrations (e.g. 100, 500, 1000, 5000 and 10000 ppm) in synthetic air at room temperature. The sensor showed 484.1% response magnitude with 21.04s and 47.09s response and recovery time at 100 ppm H<sub>2</sub>. A comparative study explaining the role of rGO-ZnO heterojunction co-relating the experimental findings has also been presented. The physics behind this room temperature sensing has been discussed thoroughly with supportive band diagram.

**Index Terms**—High sensitivity, Hydrogen, Nanohybrid structure, rGO-ZnO NPs, Room temperature

## I. INTRODUCTION

Hybridization of nanostructured metal oxides with graphene has been well documented due to its supportive chemical and physical properties like large surface area, high mobility and chemical stability [1, 2]. Sporadic attempts have been made by many researchers [3, 4] to study the semi metal behavior of graphene where they found that the low resistivity of graphene is a serious problem in the application of gas sensor. To overcome this issue, graphene and its derivative paved a new way in the area of next generation gas sensors. There are various methods have been adapted to optimize the sensing parameters like response magnitude, response time and

The work of S. Das was supported by IISER, Nadia, Chemistry and physics department and Indian Institute of Technology Roorkee. The associate editor coordinating the review of this paper and approving it for publication was Prof. C.K. Sarkar, T. S. Bhattacharya (*Corresponding author: Sunipa Roy.*) The authors are with the IC Design and Fabrication Centre, Department of Electronics and Telecommunication Engineering, Jadavpur University, Kolkata.700032, India (e-mail: [sunipa\\_4@yahoo.co.in](mailto:sunipa_4@yahoo.co.in) and [swapan\\_1976@yahoo.co.in](mailto:swapan_1976@yahoo.co.in)).

Prof. C.K. Sarkar author is presently associated with IEST, Shibpur and Howrah 711103, India (e-mail: [phyhod@yahoo.co.in](mailto:phyhod@yahoo.co.in)).

Mr. T. S. Bhattacharya Author was associated with Bose Institute, Kolkata 700009 and India (e-mail: [tarashankar1992@gmail.com](mailto:tarashankar1992@gmail.com)).

recovery time. Reduced graphene oxide is a good alternative due to its higher resistivity, inherited high mobility and other interesting property.

Literature survey [5-9] reveals that the sensing performance of rGO-ZnO nanocomposite towards H<sub>2</sub> and other reducing gases improved significantly by incorporating rGO-ZnO nanohybrid structure either in distinct layers or in the form of composite as it provide unrestricted flow of electrons one to another.

Sensing performance of any metal oxide sensors like ZnO is the function of working temperature [10]. The high working temperature leads to higher power consumption, additional fabrication steps and imposes several restrictions on its performance like poor selectivity. The depletion layer that appears around the ZnO grain boundaries opposes the electrons transfer thus degrading the response of the sensor.

To circumvent the above mentioned problems, several modifications like doping or surface fictionalization have been adopted. Literature review [5-9] reveals that the sensing performance of ZnO towards hydrogen was found to be improved extensively by integrating rGO nanosheets at some optimum temperature. But there is a crisis of room temperature hydrogen sensor with higher response and faster response/recovery time. As for example, Zain et al. [5] reported the rGO-loaded ZnO composite NFs and rGO-loaded SnO<sub>2</sub> composite NFs that were exposed to H<sub>2</sub> gas of 10 ppm concentration at 300°C temperatures. With 10 ppm H<sub>2</sub> rGO-ZnO NFs revealed greater responses than the rGO-loaded SnO<sub>2</sub> NFs at 300°C which is quite high.

Vardan et al. [6] was prepared a hybrid structure based on GO and ZnO on alumina substrate. It has been proved by that rGO /ZnO composites showed 40-50% enhanced response to NO<sub>2</sub> and H<sub>2</sub> over pure ZnO sensors. But the drawback of this method is its incompatibility to standard CMOS process technology.

Similarly, Dongzhiet. al. [7] has reported a hybrid structure of e ZnO/ rGO prepared by hydrothermal process and its use as methane gas sensor. The sensor exhibited outstanding repeatability, fast response-recovery time (30s and 40s) with good selectivity, at as low as 190 °C temperature. But the work used a built in Ni-Cr microheater which require additional fabrication steps.

Kanika et al. [8] also prepared Graphene/zinc oxide (ZnO) nanocomposite on alumina substrate by in situ reduction of zinc acetate ((CH<sub>3</sub>COO)<sub>2</sub>Zn·2H<sub>2</sub>O) and graphene oxide (GO) during refluxing. Sensor revealed that at 1.2 wt%



# Arduino Based Hand Gesture Control of Computer

Ayushi Bhawal<sup>1</sup>, Debaparna Dasgupta<sup>2</sup>, Arka Ghosh<sup>3</sup>, Koyena Mitra<sup>4</sup>, Surajit Basak<sup>5</sup>

Department of Electronics and Communication Engineering  
Guru Nanak Institute of Technology, India

## Abstract:

Gesture based interaction systems are becoming very popular both at workplace and home. This work intends to develop a system which can recognize hand gestures which can be used as an input command to interact with the PC or laptop. One of the key areas which need to be looked at while developing such systems is the code implementation stage. In order to manage the work we shall be using Python for the implementation of the code. We feel that if we successfully meet our goals then we shall have contributed towards the future of natural gesture based interfaces, if only in a minimal way.

**Keywords:** Hand gesture, Ultrasonic sensors, Arduino UNO, Python.

## I. INTRODUCTION

In order to control pc using ultra sonic sensors, this technique is called Leap motion which enables us to control certain functions on our computer/Laptop by simply waving our hand in front of it. It is very cool and fun to do it, but these laptops are really priced very high. So in this work let us try building our own Gesture Control Laptop/Computer by combining the power of Arduino and Python. We will use two Ultrasonic sensors to determine the position of our hand and control a media player (VLC) based on the position. We have used this for demonstration, but once we have understood the work, we can do anything by just changing few lines of code and control our favourite application in our favourite way. The concept behind this work is very simple. We will place two Ultrasonic sensors on top of our monitor and will read the distance between the monitor and our hand using Arduino, based on this value of distance we will perform certain actions. To perform actions on our computer we use Python Pyautogui library. The commands from Arduino are sent to the computer through serial port. This data will be then read by python which is running on the computer and based on the read data an action will be performed. The incoming time-domain signals are buffered, and Fourier transform is applied on them. The Arduino can be connected to the PC/Laptop for powering the module and also for serial communication. The result of this operation is magnitude vectors that are spread equally over the spectral width. After each FFT vector is computed, it is further processed to determine the bandwidth of the signals, speed of gestures and motion detection. The detected motions are then converted to pc commands.

### A. Proposed Work

This paper introduces a technique based on determining distance by the sensor and accordingly a particular function is performed. Some recognition methods of the gestures are proposed and then actions are recognized using sensor. We set up few mainstream methods based on the action recognition by the sensors. The sensor device is attached on computer at head of the screen, for quick operation. In this field much research work has been done but that work is related to hand recognition, real time finger

recognition and recognition of alphabet characters [1]. Real time human computer interactions using hand gesture are also used for much functionality [2] such as video control, music player, gaming [2], controlling the functions of PDF reader etc. All these interactions have real time gesture recognition techniques. A gesture controller resolution always requires a physical device which follows and recognizes the body languages or movements, so that the computer can clarify them [3]. By using ultrasonic sensor, the distance of hand can be found which acts as aninput. According to the distance of hand, particular function is performed.

## II. SYSTEM MODEL

### A. Principle Behind Our Proposed Scheme

The principle behind the Arduino based Hand Gesture Control of Computer is basically very simple. All we have to do is use two Ultrasonic Sensors with Arduino, place our hand in front of the Ultrasonic Sensor and calculate the distance between the hand and the sensor. Using this information, certain actions in the computer can be performed. The position of the Ultrasonic Sensors is very significant. The two Ultrasonic Sensors are to be placed on the top of a laptop screen at either end. The distance informations from Arduino are collected by a Python Program and a special library called PyAutoGUI will convert the data into keyboard click actions.

### B. Circuit Diagram

The circuit diagram of Arduino part of the model is shown in the figure 1. It consists of an Arduino UNO board and two Ultrasonic Sensors. We can power up all these components from the laptop's USB Port.

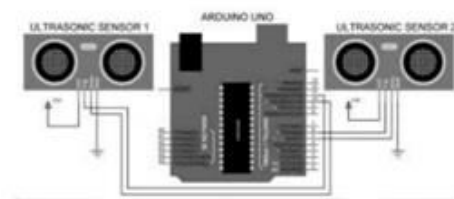


Figure.1. Circuit diagram of system



# International Journal of Modern Engineering and Research Technology

Website: <http://www.ijmert.org>

Email: [editor.ijmert@gmail.com](mailto:editor.ijmert@gmail.com)

## A CPW fed Modified Ring Patch Antenna with DGS for Multi Frequency & Wideband Wireless Communications

**Anurima Majumdar**

*M.Tech. Research Scholar*

*Department Of Electronics & Communication Engg.*

*Guru Nanak Institute of Technology*

*JIS Group, Kolkata, (W.B.) [INDIA]*

*Email: [anurima.majumdar@gmail.com](mailto:anurima.majumdar@gmail.com)*

**Sisir Kumar Das**

*Dean*

*Guru Nanak Institute of Technology*

*JIS Group, Kolkata, (W.B.) [INDIA]*

*Email: [dean\\_gnit@jisgroup.org](mailto:dean_gnit@jisgroup.org)*

**Annapurna Das**

*Director*

*Guru Nanak Institute of Technology*

*JIS Group, Kolkata, (W.B.) [INDIA]*

*Email: [director\\_gnit@jisgroup.org](mailto:director_gnit@jisgroup.org)*

### ABSTRACT

*This paper describes a modified ring patch antenna to obtain wide band and multifrequency responses for applications in wireless communication. Radial slots and tuning arms at the inner periphery of the ring are added for better impedance matching and enhancement of bandwidth. The antenna is fed by coplanar waveguide (CPW) and defective ground structure (DGS) is introduced by cutting two parallel slots in the ground plane. The patch is etched on FR4 epoxy dielectric substrate with dielectric constant 4.4 and thickness 1.6mm over the ground plane. Ansoft HFSS software tool is used for the simulation and modelling of the antenna and design optimization. When a simple microstrip line inset fed ring shows an impedance bandwidth ( $S_{11} < -10\text{dB}$ ) of 3% at 3.5GHz with return loss of -9dB, the modified configuration of the antenna produces multi frequency response with return loss peaks ( $\leq -15\text{dB}$ ) at 1.12GHz, 2.35GHz, 2.49GHz, 2.9GHz, 3.3GHz & 3.5GHz. In this configuration the highest impedance bandwidth of 29% is obtained in the frequency range from 2.35GHz to 3.2GHz.*

*The return losses and radiation patterns are measured using a Vector Network Analyzer. Simulation results agreed well with those of experimental ones. The antenna can be used in various applications in wireless communication.*

**Keywords:**— CPW fed patch antenna, defective ground structure, multifrequency antenna, ultra wide bandwidth antenna.

### I. INTRODUCTION

Enhancement of bandwidth is one of the most challenging works in designing a patch antenna for wireless communication applications. Several techniques are used by many authors and published in the literature. R. Chair, et. al[1] described a CPW-fed ultra wideband slot antenna with u-shaped tuning stub that shows a large impedance bandwidth in the frequency range from 5.5GHz to 22GHz. E. S. Angelopoulos, et.al [2] presented a coplanar waveguide fed circular and elliptical slotted patch with high bandwidth in the frequency range from 1.3GHz to 20GHz. A good work on CPW fed slot antenna is also reported by

# Ultra Wide Band CPW Fed Patch Antenna with Fractal Elements and DGS for Wireless Applications

Anurima Majumdar\*, Sisir K. Das, and Annapurna Das

**Abstract**—This article describes multiresonance behaviour to achieve ultra-wideband (UWB) characteristics of a co-planar waveguide (CPW) fed circular patch antenna with a ground plane reflector by using fractal elements and rectangular defective ground structure (RDGS) technique. The patch consists of a circular disc with six ring type fractal elements on the periphery of the disc and slotted defective ground surface (DGS) at the bottom of an FR4-epoxy dielectric substrate to increase the antenna bandwidth. The antenna resonates at frequencies of 5.4 GHz, 9 GHz, & 10.8 GHz with return loss better than  $-20$  dB. The proposed antenna also exhibits UWB characteristics with ( $\leq -10$  dB) impedance bandwidth of 170.4% in the frequency range from 1.8 GHz to 11 GHz. This covers the whole UWB range from 3.1 GHz to 10.6 GHz as defined by FCC. The antenna exhibits nearly omnidirectional radiation pattern and a gain ranging from 1 dBi to 6.8 dBi within the operating frequency range (1.8 GHz–11 GHz). An equivalent circuit model of the proposed antenna is developed, and the circuit response is obtained. All the measured results are found in good agreements with the simulated ones. The proposed antenna is suitable for applications in Wi-Fi, IEEE 802.11a Wireless LAN, WiMAX, ISM bands, wireless communications, etc.

## 1. INTRODUCTION

As per FCC, the UWB range is defined from 3.1 GHz to 10.6 GHz [1]. The ultra-wideband (UWB) patch antennas have advantages for its conformability, wideband operability, high data rate, low power consumption, robustness to fading, response to high speed pulses, small size, light weight, and low cost [1–5]. Many techniques have been reported in the literature for enhancing patch antenna bandwidth and multifrequency operation. One of the commonly used techniques is to configure the patch with fractal geometry [4–7]. Fractal elements are space-filling self-repeating structures that can be used in the form of Koch island, Sierpinski Carpet, Sierpinski gasket, Minkowski loop, Hilbert Curve, branches of tree, rough terrains, etc. In some recently published works Desai et al. [2] and Fallahi and Atlasbaf [3] used hexagonal shaped fractal geometries to obtain multiresonance and wideband response. The authors of both the papers used CPW feeding technique. Desai et al. [2] obtained a higher bandwidth of 135% after adding a defective ground structure which was better than that of [3]. Tripathi et al. [4] reported a hexagonal fractal antenna using Koch geometry for DGS and obtained a bandwidth of 122%. Ali et al. [7] proposed a miniaturized UWB antenna based on Sierpinski square slots and a defective ground structure. They reported a bandwidth of 124.7%. Many authors have used techniques other than fractal elements like loading of L-shaped slot and meandered line slots [8], edge tapering, and adding parasitic stubs [9], elliptic single complementary split-ring resonators (ESCSRRs) [10], split ring resonator [11], using of parasitic units [12, 13], step impedance resonator (SIR) [14, 15], to achieve multifrequency and UWB response. The usage of fractal elements is advantageous due to their behaviour as interconnected

---

*Received 30 April 2019, Accepted 8 July 2019, Scheduled 22 July 2019*

\* Corresponding author: Anurima Majumdar (anurima.majumdar@gmail.com).

The authors are with the Department of Electronics and Communication Engineering, Guru Nanak Institute of Technology, JIS Group, Kolkata, West Bengal 700114, India.



## Regular paper

## Multifrequency rectangular microstrip antenna with array of L-slots

Antara Ghosal\*, Sisir Kumar Das, Annapurna Das

Department of Electronics and Communication Engineering, Guru Nanak Institute of Technology, Kolkata, West Bengal 700114, India  
Maulana Abul Kalam Azad University of Technology, West Bengal, India

## ARTICLE INFO

## Article history:

Received 5 May 2019

Accepted 28 August 2019

## Keywords:

Coaxial feed

Multi frequency antenna

Slotted microstrip patch antenna

## ABSTRACT

A rectangular microstrip antenna containing an array of narrow L-slots and inverted L-slots is described for multifrequency operation. The patch was designed for  $TM_{010}$  mode of excitation at 2.1 GHz and is fed with a coaxial probe from the ground plane. The slots are cut on the patch at two opposite corners. The widths and lengths of these slots are varied to obtain the optimum performance at multiple frequencies. The performance parameters of this antenna are reflection coefficient ( $S_{11}$ ), radiation pattern, gain, and efficiency. A simple slotted structure without any additional electronic circuit was designed for multifrequency operation. The Ansoft HFSS software tool was used for the simulation and optimum design of the antenna on a FR-4 dielectric substrate above a ground plane. It is observed that the final configuration produces very good performance at penta frequencies: 1.25, 1.48, 1.8, 2.25, and 2.9 GHz with reasonable gain. The simulation results are verified with the experimental results and are found to be in good agreement.

© 2019 Elsevier GmbH. All rights reserved.

### 1. Introduction

In recent years, the development of telecommunication technology has increased. The technology has reached to 5G through 3/4G. Subsequently challenges in the design of mobile phone antenna have increased for multiband operation. The GSM frequency bands are 850, 900, 1500, 1900, 2300, 2600 MHz, UMTS frequency bands are 1885–2025 MHz and 2110–2200 MHz. LTE and WiMax frequency bands are 700 MHz, 1700–2100 MHz, 1900 MHz and 2500–2700 MHz. Ultra-high frequency bands are 1240–1300 MHz and 2900–4100 MHz. Microstrip patch antennas are widely used in large quantities for their compact size, light weight, low profile, planar configuration, portability, robustness and low fabrication cost. But, there are some disadvantages as well. Such as narrow band, low efficiency and low gain. Slotted microstrip antennas are designed for operation at multiple frequencies for different mobile networks at different countries.

For multifrequency operations, slotted microstrip patches are used with aperture couple feed [1]. A dual frequency antenna using single co-axial feed and a pair of bent slots placed close to non radiating patch is presented and these resonant frequencies are controlled by changing the bent angle [2]. Different compact spiral microstrip antennas are described in the literature [3,4] for multiband operation in which the size of the antenna is reduced as com-

pared with that of traditional patch antenna. A patch antenna is designed for operation at hexa-band frequency by reconfiguring the shape using electronic switching [5]. Various types of modeling techniques are proposed for broad banding, multiband operation, size reduction, and circular polarization [6,7]. Formulation of the slot's resonant length in some slotted microstrip antenna are given by using surface current and voltage distributions for dual-band operation [8,9]. A gap-coupled and multilayer-stacked microstrip antenna is presented for multiband and broadband operation [10]. A dual-fed dual-frequency dielectric resonator antenna (DRA) is investigated for high gain [11]. A triple-band microstrip antenna with three-nested loop and a rectangular stub connected to the feed line with good impedance matching is proposed [12]. A complicated two-layered (including a partial reflecting surface) dual-band microstrip antenna is presented [13]. A slotted elliptical patch is designed for multifrequency operation and an inset-fed dual-band patch antenna array with DGS is proposed [14,15].

A slotted array antenna using cavity-backed substrate integrated waveguide (SIW) for dual-band operation is investigated [16]. The operation mechanism of high-order modes is analyzed and then verified through simulations by inserting metallic vias in different positions of the resonant SIW cavity. A complicated antenna structure with T-shaped SLRR (Stub Loaded Ring Resonator) slot on the ground plane is designed. Also a U-shaped slot on microstrip feed line is there. The antenna is investigated for dual-band and triple frequency operation with wide bandwidth [17]. Some slotted triangular microstrip patch antennas with mul-

\* Corresponding author.

E-mail address: [antara.ghosal1989@gmail.com](mailto:antara.ghosal1989@gmail.com) (A. Ghosal).

# IoT Based Auto-Irrigation System for Agriculture

Avirup Mondal, Bikram Saha, Ananya Biswas, Anurima Majumdar, Antara Ghosal

**Abstract:** This paper describes a cost-effective water saving IoT based intelligent irrigation system for agriculture. Today, the farmers are suffering from the lack of resources, rains and scarcity of water. The objective of this paper is to design a smart irrigation system that would be useful for water management. In this IoT based system a moisture sensor is used to sense the moisture content present in the soil and according to that the water irrigation will be controlled by a microcontroller. A filter is also introduced for the purification of water as per requirement. There is no need of GSM modules or any wireless transmission gateway which makes the cost of the system around Rs. 1000/- which makes it economically affordable for Indian farmers. So, there is a need of saving water for which we need a smart technology that is an intelligent irrigation system that will help us to manage the usage of water in agriculture.

**Index Terms:** IoT, Smart Agriculture

## I. INTRODUCTION

In countries like India agriculture is an important part of socio-economic balance. According to the huge population of this country there is a high demand of food, which demands continuous advancement in the field of agriculture and technology. To maintain good agricultural system, maintenance of the fertility of soil and irrigation management are the two most important things. Water management specially in case of irrigation is a big challenge for countries like India. Nowadays for irrigation different techniques are available which are used to reduce the dependency of rain. To improve water efficiency there must be a proper irrigation scheduling strategy.

IoT offers a compact system with interconnected objects with built-in capability of computing, sensing and communication [1]. Many authors have reported smart irrigation system using microcontroller and raspberry pi [2-5]. The cost of these proposed system is on an average Rs. 15000/-. Most of them require a good network coverage and high maintenance.

**Revised Manuscript Received on June 15, 2019.**

**Avirup Mondal**, Department of Electronics & Communication Engineering, Guru Nanak Institute of Technology, JIS Group, Kolkata, West Bengal, India

**Bikram Saha**, Department of Electronics & Communication Engineering, Guru Nanak Institute of Technology, JIS Group, Kolkata, West Bengal, India.

**Ananya Biswas**, Department of Electronics & Communication Engineering, Guru Nanak Institute of Technology, JIS Group, Kolkata, West Bengal, India.

**Anurima Majumdar**, Department of Electronics & Communication Engineering, Guru Nanak Institute of Technology, JIS Group, Kolkata, West Bengal, India.

**Antara Ghosal**, Department of Electronics & Communication Engineering, Guru Nanak Institute of Technology, JIS Group, Kolkata, West Bengal, India. E-mail: [antara.ghosal1989@gmail.com](mailto:antara.ghosal1989@gmail.com)  
[/antara.ghosal@gnit.ac.in](mailto:antara.ghosal@gnit.ac.in)

During the field survey the authors came to know that many of the farmers are not equipped with smart phones and some have only one phone in the family. Many of the fertile fields are not under network coverage. Many farmers do not have idea about smart irrigation nor do have enough financial capability to afford one due to high cost.

So, the main aim of the project was to design a model that would fulfill all the auto-irrigation criteria and also would be easy to avail by the farmers.

In this paper the concept of IoT is used to design an auto-irrigation system. The main objectives are

- Improve water management
- Reduce human intervention
- Make it economically friendly to farmers
- Conservation of water.

The concept of IoT is used in the model of smart irrigation system. It helps in water conservation by automatically providing water to the agricultural field depending upon the dampness (moisture) level of soil and the temperature of nature's domain. But the great issue is water pumping based on the soil conditions. In this system an electronic device is responsible for sensing Moisture conditions. When this moisture value is not up to the required level in irrigation field then the motor is switched on to irrigate the field. Smart irrigation systems estimate and measure the existing plant moisture in order to restore water as needed while minimizing excess water use. A filter is used here to purify the water as per the requirement of the crops.

## II. MATERIALS & METHODOLOGY

### A. System Architecture

The proposed auto-irrigation system uses soil moisture sensor, power supply, DC water pump motor (9v), Arduino-Nano, water level indicator as shown in the Figure 1. The microcontroller Arduino Nano (ATmega328P) is the core part of the system. The moisture sensors are connected to the input pin of the controller. The water pump is connected with the output pin with the help of 5v relay module. If the sensors depart from the predefined range, the controller turns on the pump. The DC pump is connected with the water reservoir. The water is stored in the reservoir after filtration (if needed). There is a water level indicator with an alarm connected with the reservoir which will indicate whether the reservoirs full or not.





# Distributed Routing for Interference Minimization in Cognitive Radio Networks

Surajit Basak

Department of Electronics & Communication Engineering  
Guru Nanak Institute of Technology, Kolkata, India

## Abstract:

We investigate the problem of total interference minimization at primary user under the constraint of end-to-end data rate in cognitive radio networks. To solve the problem a cross layer approach is adopted. Closed form expression for power allocation is obtained and from which routing metric and spectrum assignment policy is also extracted. Distributed implementation related to the proposed optimal routing, power allocation and channel allocation scheme is also proposed. Simulation results show that our proposed optimal approach succeeds in reducing interference to primary user in a significant manner.

**Keywords:** Cognitive radio networks, Cross-layer, Decode-and-forward, Interference.

## I. INTRODUCTION

Cognitive radio network (CRN) [1] is a dynamic spectrum access network where communication among the nodes is carried out through the unused spectrum of licensed users available at the instant. A CRN consists of Primary Users (PUs) that have licensed spectrum bands to operate and Secondary Users (SUs) who uses the available spectrum of PUs in an opportunistic manner for communications. Most research in CRN has focused on a single-hop wireless access network, the research community has recently realized that cognitive paradigm can be applied in multi-hop networks to provide great potential for unexplored services and enable a wide range of multimedia applications with the extended network coverage. In the last few decades different routing schemes have been developed for CRNs [2-3]. However any routing scheme that increases the level of interference optimization [4] than the existing schemes will enhance the performance of the networks. Considering the PUs as prime concern the best routing scheme will result in minimum interference at PUs without any constraint on transmission rate. Recently, the issue of routing for interference minimization in multihop CRNs was studied in [5-6]. To the best of authors' knowledge, the issue of joint power allocation, routing and channel allocation in data rate restricted CRNs has not yet been considered in open literature. Therefore, in this paper, we study a cross layer approach with the core objective of interference minimization, which has great importance from the perspective of green communication. To solve the problem, first we propose joint power allocation, routing and channel allocation strategy in CRNs for solving the minimum interference problem for a given end-to-end data rate constraint. The solution may be described in three parts. First, a closed form solution for power allocation is obtained for this joint optimization problem with end-to-end data rate constraint. Next, we design a novel path weight function and channel allocation strategy. Further distributed implementation is also proposed for the optimal scheme. This is the main contribution of the paper. The content of this paper is arranged as follows. The system model is described in Section II. In Section III, we design the problem for total interference power optimization under the constrained

transmission rate ( $R$ ) and derive its solution. A distributed route selection strategy, channel allocation and power allocation are proposed in Section IV. Section V presents the network performance evaluation through simulation. Finally, we conclude the paper in Section VI.

## II. SYSTEM MODEL

### A. Network Model

Let us consider a CRN consisting of  $N$  no. of SUs and  $K$  no. of PUs is located outside the network area. The network is represented by an undirected graph  $G = (V, E)$  where  $V$  denotes the set of SU nodes and  $E$  denotes the set of wireless links between SU nodes in the network. SUs are numbered from  $SU_1$  to  $SU_N$  whereas the PUs is numbered from  $PU_1$  to  $PU_K$ . Each  $PU_k$  ( $k \in 1, 2, \dots, K$ ) consists of a primary transmitter  $PT_k$  and a primary receiver  $PR_k$ . The locations of the PU nodes are fixed and the SU nodes are considered to be static or moves very slowly. For ease of understanding a single routing session is considered between a given source-destination pair. Let  $SU_1$  be the source node and  $SU_n$  is the destination node. A path is defined between the source and destination nodes by a sequence of connected nodes where no node is encountered more than once. The path  $p = \langle SU_1, SU_2 \dots SU_i \dots SU_n \rangle$ , where  $SU_i$  ( $i \in 2, 3, \dots, n-1$ ) acts as decode-and-forward (DF) relay nodes.

### B. Wireless Link Model

We consider that the wireless links between the SU nodes are Rayleigh distributed and the fading amplitudes are statistically independent to each other. We assume that the network is using time division multiple access protocol (TDMA) without spatial reuse and noise at each SU node is Additive White Gaussian Noise (AWGN) with zero mean and unit variance. In our system model, only the interference to the PRs due to SU nodes are taken into account. The interference to the SU nodes due to PRs are ignored. The channel gain from  $SU_i$  to  $PR_k$  is determined by

$$h_{i,k}^{sp} = \beta \max [d_{min}, d_{i,k}]^{-\alpha/2} \quad (1)$$

# Stability and Control of Quadcopter

Tanusri Roy<sup>1</sup> Stuti Ghosh<sup>2</sup> Titas Ghosh<sup>3</sup> Srijoni Malakar<sup>4</sup> Avali Banerjee<sup>5</sup>

<sup>1,2,3,4,5</sup>Department of Electronics & Communication Engineering

<sup>1,2,3,4,5</sup>Guru Nanak Institute of Technology, 157/F Nilgunj Road, Sodepur, Kolkata, India

**Abstract**— This project presents a systematic approach towards the stability analysis and control of a real dynamic system. A very interesting mechatronics platform, namely, quadrotor helicopter, which is a highly nonlinear and cross-coupled dynamic system and poses challenges for many classical control techniques, has been considered as a candidate system to illustrate the proposed control law. A novel methodology has been presented to analyze the stability of the nonlinear system by using Lyapunov- Krasovskii method and stabilize the system by implementing the control law. Lyapunov-Krasovskii method for analyzing the stability offers distinct advantages over other control methods. PD and PID control law have been implemented to stabilize the system and produce satisfactory results. Therefore, PD and PID controller can make quadcopter approaching the stationary state.

**Key words:** Quadrotor, Nonlinear System, Cross-Coupled Dynamic System, Lyapunov- Krasovskii Method, Quadcopter

slow spinning motor, which enables it to roll and pitch. Roll and pitch angles divide the thrust into two directions due to which linear motion is achieved. The rotors rotate in clockwise- anticlockwise pairs, shown in Fig. 3 to control the yaw produced due to the drag force on propellers. The Center of Gravity (CG) lies almost at the same plane which contains all the rotors. Also, all four motors of same class differ in efficiency with each other. This differentiates it from the helicopters, and it is very difficult to stabilize a quadcopter by human control. Therefore, sophisticated control is essential for a balanced flight of quadcopter.

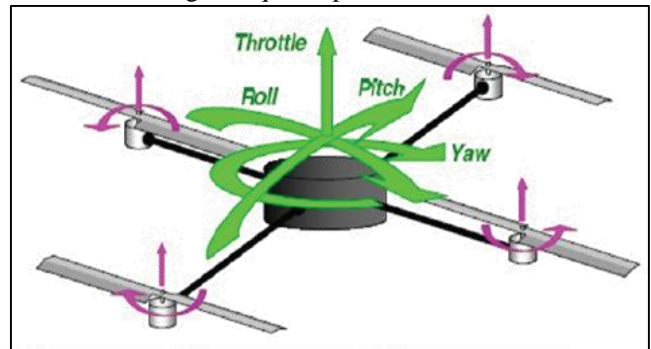


Fig. 1: Quadcopter

## I. INTRODUCTION

In recent year there has been widespread interest in the small unmanned aerial vehicles (UAV) utilized in various civilian applications, like weather analysis, delivery services, news agencies, traffic management and also used in a different military operation like aerial surveillance, information gathering, and aerial targeting. Therefore, an unmanned aerial vehicle is an interesting mechatronics system and poses significant challenges for the application of many conventional control design technique. One of the most popular types UAV commercially used in the civilian application is Quadcopter. One of the most popular types UAV commercially used in the civilian application is Quadcopter. The quadcopter has received extensive attention from the researchers for the aerodynamic properties have been incorporated in mathematical modeling, makes it more complicated for precise and stable control. . Therefore, any attempt to derive a generalized state-space model for such a nonlinear and coupled multivariable system results in a very big and complex mathematical model. The main purpose of this project is to present the basis of quadcopter modeling and control to form a basis for further research and development in the area. This project pursued with two aims, the first aim is to study the mathematical modeling of the quadcopter for analyzes the stability of the system and the second aim is to implement an appropriate control law for stabilization and trajectory control of the candidate system.

## II. MODELING OF A QUADCOPTER DYNAMICS

A quadcopter is a four-rotor helicopter. It is an under actuated, dynamic vehicle with four input forces (one for each rotor) and Six Degrees of Freedom (6DOF). The motion of a quadcopter in 6DOF is controlled by varying the rpm of the four rotors individually, thereby changing the lift and rotational forces quadcopter tilts toward the direction of the

## III. BASIC MOVEMENTS MODELING AND SIMULATION USING HFFS

The motion of quadcopter in 6DOF is controlled by varying the rpm of four rotors individually. According to the rotor number 1 and 3 (or front and rear rotor) rotates CCW (Counter Clock Wise), and rotor number 2 and 4 (or right and left rotor) rotates CW (Clock Wise). Because of this arrangement, aerodynamic torque is canceled by each other. Initially, the helicopter is on the ground before taking off. There are five status of movement condition for the quadrotor helicopter after taking-off. Those are hovering, vertical (or thrust), rolling, pitching and yawing movements. Each movement condition is characterized by different motor speeds.

### A. Hovering

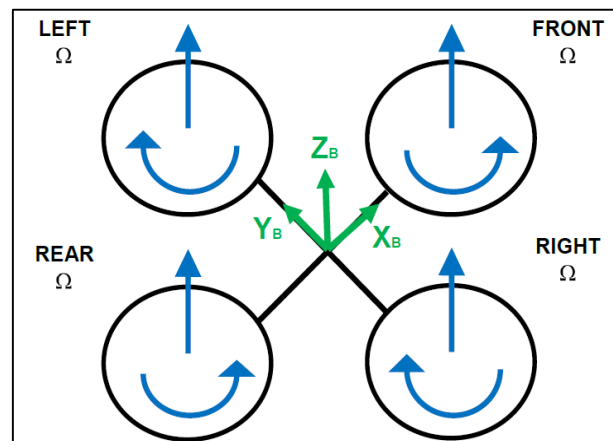


Fig. 2: Quadcopter Schematic (Hovering)



# On BER Minimizing Routing and Power Allocation in Multi-Hop Cognitive Radio Ad-Hoc Networks

Poulomi Das<sup>1</sup>, Pratyasha Mitra<sup>2</sup>, Ankita Pal<sup>3</sup>, Kaustuva Chakraborty<sup>4</sup>, Surajit Basak<sup>5</sup>  
Department of Electronics & Communication Engineering  
Guru Nanak Institute of Technology, Kolkata, India

## Abstract:

Route selection to minimize end-to-end (e2e) bit error rate (BER) experienced by secondary users (SUs) in a given communication session is one of the key challenge in a multi-hop CRAHN. We study the problem under the constraint of total interference power at primary receiver due to the transmission of SUs. The above problem is formulated as a joint power allocation and routing problem. By using Lagrangian convex optimization, closed form expression for optimal power allocation is obtained for SU source and relay nodes. Based on that, path weight function and routing metric is extracted. Distributed implementation of the proposed joint power allocation and routing scheme is also presented. Simulation results show that our proposed scheme succeeds in BER minimization in a significant manner.

**Keywords:** Cognitive radio ad hoc networks; BER minimization interference minimization; multi-hop; joint routing and power allocation.

## I. INTRODUCTION

Cognitive radio (CR) has emerged as a potential solution for the problem of spectrum scarcity by implementing dynamic spectrum access (DSA) technology [1]. In CR system, secondary users (SUs) are allowed to access the licensed spectrum, originally allocated by primary user (PU), without compromising the interest of PU. CR networks are of two types: infrastructure based networks and infrastructure less networks. The second type is known as CR ad hoc networks (CRAHNs) [2]. Routing in CRAHNs is a challenging task because existing routing solutions for wireless ad-hoc networks (WANETs) fall short of meeting the unique routing challenges in such networks that includes dynamic nature of spectrum availability due to stochastic presence of PUs in the licensed band. In [3], the authors propose a distributed routing and scheduling algorithm to minimize the cumulative interference to PU by adaptively updating the individual link cost by interference to PU from corresponding SU and flow condition. In [4], the authors adopt a game-theoretic approach for designing a distributed and dynamic routing scheme for minimizing both overall interference from the SUs to the PUs. In [5], authors propose a power control mechanism to minimize aggregate interference at PU in underlay CR networks. In previous paper author developed two new joint power allocation and routing strategies: minimum total power (MTP) strategy and equal power allocation (EPA) strategy. While objective function for MTP is the total power which is to be minimized for BER constraint, EPA strategy provides maximum path life time for the BER constraint. In previous paper author investigate the problems of SUs networks lifetime maximization and interference to PU minimization jointly in BER constrained stationary ad hoc networks. To the best of our knowledge none of the earlier above studies BER minimizing routing CR networks. In this paper, a routing problem is formulated to minimize the end-to-end (e2e) BER in CRAHNs. Considering the issues of transmit power allocation, interference to the primary receiver (PR) and BER together in CRAHNs, it may be noted that increase in transmit power leads to decrease in e2e BER but it enhances

interference to PR. Thus, we aim to find a route that minimizes e2e BER with the constraint of total interference at PR caused by the transmission of SUs. First, closed form expression for power allocation is obtained. From this power allocation solution, a novel path weight function is obtained which is shown to satisfy three essential properties of any routing protocol i.e. optimality, convergence and loop freeness. A modified distributed Bellman-ford algorithm is applied to find the optimal route. Simulation results are also present to verify our analysis. The remainder of the paper is organized as follows. Immediate next section introduces system model with key assumptions. The problem is also formulated in this section. Section 3 represents closed form expression of power allocation solution followed by extraction of routing metric. In section 4, distributed implementation of routing and power allocation is presented and section 5 presents simulation results. Finally, section 6 concludes the paper.

## II. SYSTEM MODEL

### A. Network Model

Let a wireless multi hop CRAHN is modeled by an undirected graph  $G(V, E)$  where,  $V$  is the vertex set indicating the set of  $|V|$  SU nodes in the network and  $E$  indicates the edge set of the wireless links of the network. Each SU node is equipped with an omnidirectional antenna and limited battery energy. A sequence of messages is continuously transmitted by the source SU node  $S_1$  to the destination SU node  $S_{N+1}$  through a path  $\rho = \langle S_1, S_2, \dots, S_{N+1} \rangle$  with  $N+1$  ( $N+1 \leq |V|$ ) nodes where  $S_2$  to  $S_{N+1}$  nodes are the SU nodes performing the role of decode-and-forward (DF) relays. There are  $(N - 1)$  hops in the path  $\rho$  and the link between SU node  $S_i$  and  $S_{i+1}$  is denoted as  $i$ -th hop for  $i \in \{1, 2, \dots, N-1\}$ . SU nodes  $\notin \rho$  are kept in sleep mode to save energy resource. The PU network is composed of one primary transmitter (PT) and one PR is located outside the SU network area.

### B. Wireless Channel Model

We assume that the wireless links between SU nodes are characterized by large scale path loss with Rayleigh fading

# Stability and Control of Quadcopter

Tanusri Roy<sup>1</sup> Stuti Ghosh<sup>2</sup> Titas Ghosh<sup>3</sup> Srijoni Malakar<sup>4</sup> Avali Banerjee<sup>5</sup>

<sup>1,2,3,4,5</sup>Department of Electronics & Communication Engineering

<sup>1,2,3,4,5</sup>Guru Nanak Institute of Technology, 157/F Nilgunj Road, Sodepur, Kolkata, India

**Abstract**— This project presents a systematic approach towards the stability analysis and control of a real dynamic system. A very interesting mechatronics platform, namely, quadrotor helicopter, which is a highly nonlinear and cross-coupled dynamic system and poses challenges for many classical control techniques, has been considered as a candidate system to illustrate the proposed control law. A novel methodology has been presented to analyze the stability of the nonlinear system by using Lyapunov- Krasovskii method and stabilize the system by implementing the control law. Lyapunov-Krasovskii method for analyzing the stability offers distinct advantages over other control methods. PD and PID control law have been implemented to stabilize the system and produce satisfactory results. Therefore, PD and PID controller can make quadcopter approaching the stationary state.

**Key words:** Quadrotor, Nonlinear System, Cross-Coupled Dynamic System, Lyapunov- Krasovskii Method, Quadcopter

slow spinning motor, which enables it to roll and pitch. Roll and pitch angles divide the thrust into two directions due to which linear motion is achieved. The rotors rotate in clockwise- anticlockwise pairs, shown in Fig. 3 to control the yaw produced due to the drag force on propellers. The Center of Gravity (CG) lies almost at the same plane which contains all the rotors. Also, all four motors of same class differ in efficiency with each other. This differentiates it from the helicopters, and it is very difficult to stabilize a quadcopter by human control. Therefore, sophisticated control is essential for a balanced flight of quadcopter.

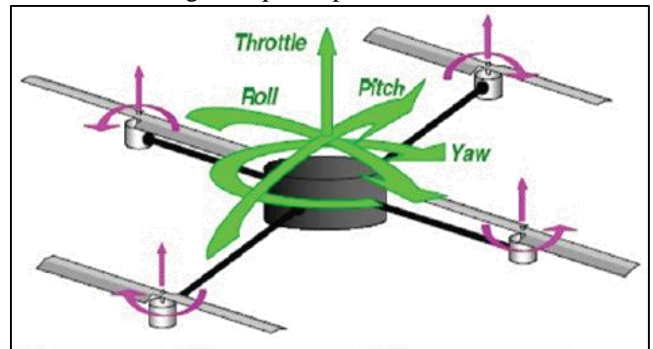


Fig. 1: Quadcopter

## I. INTRODUCTION

In recent year there has been widespread interest in the small unmanned aerial vehicles (UAV) utilized in various civilian applications, like weather analysis, delivery services, news agencies, traffic management and also used in a different military operation like aerial surveillance, information gathering, and aerial targeting. Therefore, an unmanned aerial vehicle is an interesting mechatronics system and poses significant challenges for the application of many conventional control design technique. One of the most popular types UAV commercially used in the civilian application is Quadcopter. One of the most popular types UAV commercially used in the civilian application is Quadcopter. The quadcopter has received extensive attention from the researchers for the aerodynamic properties have been incorporated in mathematical modeling, makes it more complicated for precise and stable control. . Therefore, any attempt to derive a generalized state-space model for such a nonlinear and coupled multivariable system results in a very big and complex mathematical model. The main purpose of this project is to present the basis of quadcopter modeling and control to form a basis for further research and development in the area. This project pursued with two aims, the first aim is to study the mathematical modeling of the quadcopter for analyzes the stability of the system and the second aim is to implement an appropriate control law for stabilization and trajectory control of the candidate system.

## II. MODELING OF A QUADCOPTER DYNAMICS

A quadcopter is a four-rotor helicopter. It is an under actuated, dynamic vehicle with four input forces (one for each rotor) and Six Degrees of Freedom (6DOF). The motion of a quadcopter in 6DOF is controlled by varying the rpm of the four rotors individually, thereby changing the lift and rotational forces quadcopter tilts toward the direction of the

## III. BASIC MOVEMENTSMODELING AND SIMULATION USING HFFS

The motion of quadcopter in 6DOF is controlled by varying the rpm of four rotors individually. According to the rotor number 1 and 3 (or front and rear rotor) rotates CCW (Counter Clock Wise), and rotor number 2 and 4 (or right and left rotor) rotates CW (Clock Wise). Because of this arrangement, aerodynamic torque is canceled by each other. Initially, the helicopter is on the ground before taking off. There are five status of movement condition for the quadrotor helicopter after taking-off. Those are hovering, vertical (or thrust), rolling, pitching and yawing movements. Each movement condition is characterized by different motor speeds.

### A. Hovering

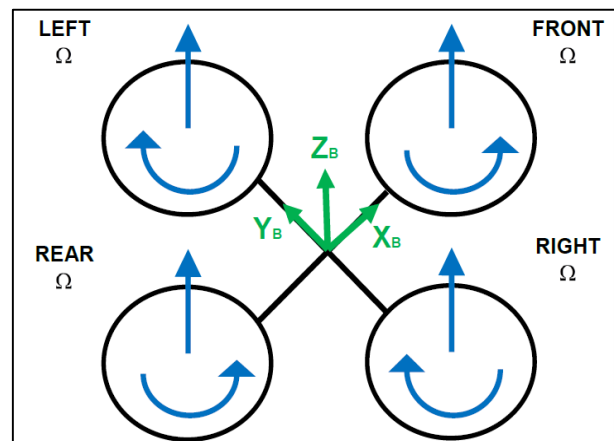


Fig. 2: Quadcopter Schematic (Hovering)

# IoT Based Auto-Irrigation System for Agriculture

Avirup Mondal, Bikram Saha, Ananya Biswas, Anurima Majumdar, Antara Ghosal

**Abstract:** This paper describes a cost-effective water saving IoT based intelligent irrigation system for agriculture. Today, the farmers are suffering from the lack of resources, rains and scarcity of water. The objective of this paper is to design a smart irrigation system that would be useful for water management. In this IoT based system a moisture sensor is used to sense the moisture content present in the soil and according to that the water irrigation will be controlled by a microcontroller. A filter is also introduced for the purification of water as per requirement. There is no need of GSM modules or any wireless transmission gateway which makes the cost of the system around Rs. 1000/- which makes it economically affordable for Indian farmers. So, there is a need of saving water for which we need a smart technology that is an intelligent irrigation system that will help us to manage the usage of water in agriculture.

**Index Terms:** IoT, Smart Agriculture

## I. INTRODUCTION

In countries like India agriculture is an important part of socio-economic balance. According to the huge population of this country there is a high demand of food, which demands continuous advancement in the field of agriculture and technology. To maintain good agricultural system, maintenance of the fertility of soil and irrigation management are the two most important things. Water management specially in case of irrigation is a big challenge for countries like India. Nowadays for irrigation different techniques are available which are used to reduce the dependency of rain. To improve water efficiency there must be a proper irrigation scheduling strategy.

IoT offers a compact system with interconnected objects with built-in capability of computing, sensing and communication [1]. Many authors have reported smart irrigation system using microcontroller and raspberry pi [2-5]. The cost of these proposed system is on an average Rs. 15000/-. Most of them require a good network coverage and high maintenance.

**Revised Manuscript Received on June 15, 2019.**

**Avirup Mondal**, Department of Electronics & Communication Engineering, Guru Nanak Institute of Technology, JIS Group, Kolkata, West Bengal, India

**Bikram Saha**, Department of Electronics & Communication Engineering, Guru Nanak Institute of Technology, JIS Group, Kolkata, West Bengal, India.

**Ananya Biswas**, Department of Electronics & Communication Engineering, Guru Nanak Institute of Technology, JIS Group, Kolkata, West Bengal, India.

**Anurima Majumdar**, Department of Electronics & Communication Engineering, Guru Nanak Institute of Technology, JIS Group, Kolkata, West Bengal, India.

**Antara Ghosal**, Department of Electronics & Communication Engineering, Guru Nanak Institute of Technology, JIS Group, Kolkata, West Bengal, India. E-mail: [antara.ghosal1989@gmail.com](mailto:antara.ghosal1989@gmail.com)  
[/antara.ghosal@gnit.ac.in](mailto:antara.ghosal@gnit.ac.in)

During the field survey the authors came to know that many of the farmers are not equipped with smart phones and some have only one phone in the family. Many of the fertile fields are not under network coverage. Many farmers do not have idea about smart irrigation nor do have enough financial capability to afford one due to high cost.

So, the main aim of the project was to design a model that would fulfill all the auto-irrigation criteria and also would be easy to avail by the farmers.

In this paper the concept of IoT is used to design an auto-irrigation system. The main objectives are

- Improve water management
- Reduce human intervention
- Make it economically friendly to farmers
- Conservation of water.

The concept of IoT is used in the model of smart irrigation system. It helps in water conservation by automatically providing water to the agricultural field depending upon the dampness (moisture) level of soil and the temperature of nature's domain. But the great issue is water pumping based on the soil conditions. In this system an electronic device is responsible for sensing Moisture conditions. When this moisture value is not up to the required level in irrigation field then the motor is switched on to irrigate the field. Smart irrigation systems estimate and measure the existing plant moisture in order to restore water as needed while minimizing excess water use. A filter is used here to purify the water as per the requirement of the crops.

## II. MATERIALS & METHODOLOGY

### A. System Architecture

The proposed auto-irrigation system uses soil moisture sensor, power supply, DC water pump motor (9v), Arduino-Nano, water level indicator as shown in the Figure 1. The microcontroller Arduino Nano (ATmega328P) is the core part of the system. The moisture sensors are connected to the input pin of the controller. The water pump is connected with the output pin with the help of 5v relay module. If the sensors depart from the predefined range, the controller turns on the pump. The DC pump is connected with the water reservoir. The water is stored in the reservoir after filtration (if needed). There is a water level indicator with an alarm connected with the reservoir which will indicate whether the reservoirs full or not.



[Home](#) > [Journals & magazines](#) > [IET Circuits, Devices & Systems](#) > [Volume 12, Issue 4](#) > Article

## Development of integrated microsystem for hydrogen gas detection

Author(s): [Swapan Das](#)<sup>1</sup>; [Chandan K. Sarkar](#)<sup>2</sup>; [Sunipa Roy](#)<sup>1</sup>

[View affiliations](#)

Source: [Volume 12, Issue 4](#), July 2018, p. 453 – 459

DOI: [10.1049/iet-cds.2017.0243](#), Print ISSN: 1751-858X,

Online ISSN: 1751-8598

[Access Full Text](#)

[Recommend Title  
Publication to  
library](#)

- [« Previous Article](#)
- [Table of contents](#)
- [Next Article »](#)

© The Institution of Engineering and Technology

Received [05/07/2017](#), Accepted [30/01/2018](#), Revised [07/12/2017](#), Published [05/02/2018](#)

### Article

A low-power microelectromechanical system-based metal–oxide gas sensor along with integrated signal conditioning unit is presented in this study to detect and quantify the variation of H<sub>2</sub> gas concentrations. The interface circuit controls the sensor operating temperature, measures the H<sub>2</sub> gas concentration, contributes a user-friendly interface and can be used with any suitable sensor network. A PIC16F877A microcontroller has been used for this purpose. The temperature of the sensors was stabilised by controlling the actuating voltage of the microheater. Temperatures of the microheater depend on the output voltage of the digital-to-analogue converter (DAC) and were measured by sampling the heater resistance through the use of a voltage divider and analogue-to-digital converters (ADCs). A microcontroller accordingly adjusts the output of DAC's in order to apply the appropriate steering voltage to the heaters. The method employed to measure the concentration of gases is to sample the voltage drop over the resistances of the sensors by ADCs. Alarming system for safety measure was also implemented in this design. The preventive action was taken by introducing an additional feature of wireless communication by sending short message service via global system for mobile modem to the designated emergency number.

Inspec keywords: [temperature measurement](#); [chemical variables measurement](#); [microcontrollers](#); [low-power electronics](#); [signal conditioning circuits](#); [gas sensors](#); [analogue-digital conversion](#); [temperature sensors](#); [microsensors](#); [voltage dividers](#)

Other keywords: [alarming system](#); [H2](#); [integrated microsystem](#); [integrated signal conditioning unit](#); [gas concentration measurement](#); [low-power microelectromechanical system](#); [voltage divider](#); [microheater](#); [mobile modem](#); [digital-to-analogue converter](#); [analogue-to-digital converters](#); [ADC](#); [interface circuit controls](#); [hydrogen gas detection](#); [metal-oxide gas sensor](#); [heater resistance](#); [actuating voltage control](#); [voltage drop](#); [DAC](#); [PIC16F877A microcontroller](#); [wireless communication](#)

Subjects: [MEMS and NEMS device technology](#); [Signal processing and conditioning equipment and techniques](#); [Thermal variables measurement](#); [Thermometry](#); [Chemical sensors](#); [A/D and D/A converters](#); [Chemical variables measurement](#); [Chemical sensors](#); [Microprocessors and microcomputers](#); [Microsensors and nanosensors](#); [Micromechanical and nanomechanical devices and systems](#); [Other analogue circuits](#)

### References

- 1) Baroncini, M., Placidi, P., Cardinali, G.C., et al: 'A simple interface circuit for micromachined gas sensors', *Sens. Actuators A*, 2003, **109**, pp. 131–136.

# Modeling of Via Interconnect through Pad in Printed Circuit Board

Avali Ghosh, Sisir Kumar Das, and Annapurna Das

Guru Nanak Institute of Technology  
JIS Group, 157/F, Nilgunj Road, Sodepur, Kolkata-700114, India  
avalighosh@gmail.com, dean\_gnit@jisgroup.org, director\_gnit@jisgroup.org

**Abstract** — In this paper the methods of finding inductance  $L$  of a cylindrical via and capacitance  $C$  due to via pad in printed circuit board (PCB) are described. Initially a thin cylindrical via of diameter  $d$  without pad is connected between a 50 ohm copper trace on the top of a dielectric substrate and a ground plane at the bottom. The line is terminated with matched load. The geometrical structure is simulated using Ansoft HFSS software tools to find the input reflection coefficient  $S_{11}$ . The value of inductance of the via is determined in terms of  $S_{11}$  using transmission line formulation. The theoretical and experimental results for  $L$  as a function of  $d$ ,  $h$ , and  $d/h$  are compared with those obtained from empirical formulae developed by the other authors. The results are found in good agreement. Secondly a square via pad is added in the trace in absence of via. The equivalent capacitance  $C$  of the pad is calculated in the same way from  $S_{11}$  as it is done for  $L$ . Finally, the PCB model is configured with a cylindrical via connected between the pad in the trace and the ground plane. The complex load impedance values are obtained from the electrical equivalent circuit of the L-C combination. This impedance is also determined from the  $S_{11}$  parameter using HFSS.

**Index Terms** — Microstrip, PCB, reflection coefficient, via, via-pad.

## I. INTRODUCTION

Vias are commonly used in PCB design to interconnect traces from one layer to another layer. In high frequency region, the traces behaves as transmission lines and the via presents inductance and/or capacitance in place of a short circuit connection between the traces. The resulting discontinuity at via position produces signal reflections and problems in the return current. An equivalent inductance and capacitance of the via are evaluated by many authors [1-12] to solve the issues related to signal integrity (SI).

An empirical formula for via inductance is given by Pucel [1] considering via image in terms of physical dimensions and electrical parameters of the substrate. Goldfarb and Pucel [2] have given an empirical

formulae without considering the image for cylindrical via above a ground plane. They showed that their numerical and experimental results agree well with those obtained by Hoefer and Chattopadhyay [3]. Closed-form expressions of the resistance, capacitance, and inductance for interplane 3-D vias is described by Savidis and Friedman [4]. Wu and Fan [5] investigated crosstalk among signal vias considering various geometrical parameters. Some closed form expressions for the computation of the via capacitance is developed by Ndip et al. [6]. Ndip, et al. [7] introduced layer stack up scheme to solve electromagnetic reliability problem due to return current paths through via. A physics based via model is given by Zhang and Fan [8] at low frequency depending upon the via geometry. Hernandez-Sosa and Sanchez [9] described the method for calculating the equivalent self and mutual inductance of signal vias in parallel planes. For the performance assessment and optimization of signal integrity, the closed-form expressions for the via-pad capacitance and via- inductance is presented by Isidoro-Munoz et al. [10]. The coupling of signal from the center trace to the adjacent side traces due to radiated signal from the via is analytically described by Ghosh et al. [11-12].

This paper describes the methods of finding inductance  $L$  of a cylindrical via and capacitance  $C$  due to via pad in printed circuit board from the concepts of transmission line theory and using HFSS. Initially the model of via considered is a thin cylindrical post of diameter  $d$  connected between a 50 ohm copper trace on the top of a thin FR4 - epoxy dielectric substrate and a ground plane at the bottom without considering any presence of pad on the trace. The line is terminated with matched load. The structure is simulated using HFSS to find the input reflection coefficient  $S_{11}$ . The value of inductance is determined in terms of  $S_{11}$  using transmission line formulation. The theoretical and experimental values of  $L$  versus  $d$ ,  $h$ , and  $d/h$  matched well with those obtained from empirical formulae developed by the other authors ([2],[4]). Subsequently, the PCB structure is taken where a square via pad is introduced in the trace without presence of via. Since no via is connected, the equivalent circuit of the via pad



# Spectrum-aware outage minimizing cooperative routing in cognitive radio sensor networks

Surajit Basak<sup>1</sup> · Tamaghna Acharya<sup>1</sup>

Published online: 13 October 2018  
© Springer Science+Business Media, LLC, part of Springer Nature 2018

## Abstract

This paper investigates the optimal path selection problem for end-to-end (e2e) outage probability minimization in clustered cognitive radio sensor networks. In order to improve outage performance of the optimal path, under a high node density regime, we consider feasibility of virtual multiple-input single-output (v-MISO) links in addition to conventional single-input single-output (SISO) links in the path. Since sensor nodes in such networks are allowed to access the spectrum of the primary network only in an opportunistic manner, the path selection problem is studied under the constraints of probabilistic interference to PU receivers and only single use of any PU channel along the path. The above problem is formulated as a joint hop-constrained routing, spectrum assignment and transmit power control problem. A convex optimization framework is used to find a closed form expression for the optimal transmit power of each transmitting node along the optimal route. Extension of the analytical result facilitates design of a novel routing algorithm, called spectrum aware-minimum outage intelligent cooperative routing (SA-MOICR) algorithm, which not only selects the minimum outage path for a given routing session, but also determines the number of nodes and the unique PU channel to be used for transmission in each hop along the path. Simulation results are found to corroborate our analytical results and quantify the significant improvement of the SA-MOICR scheme over only SISO or only v-MISO based routing solutions in terms of the achievable e2e outage probability.

**Keywords** Cognitive radio sensor networks · Cross-layer approach · Cooperative routing · End-to-end (e2e) outage probability

## 1 Introduction

Cognitive radio (CR), popular as the key technology for implementing *dynamic spectrum access* (DSA) [1], has been considered as a promising technique to improve the spectral efficiency in the next-generation wireless networks. In a CR network (CRN), secondary users (SUs) opportunistically access the licensed spectrum of one or more primary users (PUs) in such a way that the interest of the latter is well protected. Wireless sensor networks

(WSNs) typically consist of a collection of energy-limited sensor nodes working together for a common task [2]. Communication protocols in WSNs have been primarily focusing on improving energy-efficiency of the networks considering data communications. However, many new and interesting applications of WSNs are being explored, which demand efficient multimedia communications such as observing and gathering audio, image and video information from the event field [3, 4]. For this delay-sensitive real-time traffic, outage probability is a popular metric to evaluate the reliability of the transmission. But improving outage performance of any wireless fading link requires higher transmission power. Thus, design of energy-efficient communication scheme, aiming outage probability minimization in WSNs, assumes importance.

WSNs, traditionally known to operate over the license-free spectrum, are increasingly facing the problem of spectrum scarcity due to the growing congestion in the

---

✉ Tamaghna Acharya  
t\_acharya@telecom.iiests.ac.in  
Surajit Basak  
surajit.basak2007@gmail.com

<sup>1</sup> Department of Electronics and Telecommunication Engineering, Indian Institute of Engineering Science and Technology, Shibpur 711103, India

# Interference Effects of Via Interconnect in Three Layer Printed Circuit Board

Avali Ghosh, Sisir Kumar Das, and Annapurna Das

Guru Nanak Institute of Technology  
 JIS Group, 157/F, Nilgunj Road, Sodepur, Kolkata-700114, India  
 avalighosh@gmail.com, dean\_gnit@jisgroup.org, director\_gnit@jisgroup.org

**Abstract** — Cylindrical vias are commonly used for interconnection in multilayered Printed Circuit Board (PCB) design. The RF current through vias causes radiated interference to adjacent traces. This paper describes an analytical method of computing the radiation from cylindrical via using the electromagnetic theory. Three layer printed circuit board consisting of three traces on the top of a dielectric substrate, a middle orthogonal trace and a ground plane at the bottom, is considered. The RF voltage coupling at the terminations of the traces due to the near field radiation from the via is computed. The reactive couplings between the traces are determined from the parasitic elements using transmission line equations. The total coupling obtained from analytical method is compared with those of modeling and simulation with Ansoft HFSS software tool. The total crosstalk is also measured using an available Network Analyzer. A good agreement is found. The changes of radiated coupling with the change of position of via, trace separation and trace length are also investigated. This paper shows that the analytical method is a useful tool for predicting interference in PCB without using expensive simulation software.

**Index Terms** — Crosstalk, electromagnetic compatibility, PCB, transmission line, via, via inductance.

## I. INTRODUCTION

Analysis of reactive cross-talk between the traces in multilayer printed circuit board is described by Paul [1] using transmission line theory and results are well documented. In multilayer PCB, vias are placed to interconnect signals from one layer to another. Their locations are optimized for desired circuit operation with signal integrity and Electromagnetic Compatibility (EMC). Very costly software tools are utilized for this purpose. The effects of via interconnects are analyzed by many authors [2-12]. Pucel [2] developed an empirical formula for via inductance using image concept. Goldfarb and Pucel [3] developed empirical formula for via inductance based on measurements and numerical simulation. Cui et al. [4] described EMI problem due to via transitions through the DC power bus. Li et al.

[5] and Suntives et al. [6] have shown shielding of interference between PCB traces using an array of vias in a trace. Nam et al. [7] shown EMI mitigation in PCB using shorting vias around the signal via. Ndip et al. [8] described techniques to solve electromagnetic reliability problem due to return current paths through via by introducing layer stack up scheme. Jiang and Fan [9] has given an intrinsic via circuit model through rigorous electromagnetic analysis. Wu and Fan [10] analytically predicted crosstalk among multiple vias between infinitely large parallel planes. Pan and Fan [11] given an equivalent multi-conductor transmission line model to characterize via structures in multi-layer PCBs for signal integrity in high speed digital circuits. Isidoro-Munoz et al. [12] presented closed-form expressions for the via-pad capacitance and via-traces inductance for the performance assessment and optimization of signal integrity. None of the above publications described the analysis of radiation from via and its effects on the adjacent lines. Some results of radiation coupling from via placed in a fixed position are presented by the authors in international conferences [14,15].

In this paper the effects of via (interconnect) in a three layer PCB are described along with the reactive crosstalk between the traces. The three layer board consists of three parallel traces (Trace1, 2 and 3) on the top of a FR4 dielectric substrate (copper clad FR4 glass epoxy, S3110, CEM-1), a second layer trace (Trace 4) which is orthogonal to the top traces, and a bottom layer of ground plane as shown in Fig. 1. The single layer thickness of the substrate is  $h$  and having dielectric constant  $\epsilon_r$ . The trace 1 and trace 4 are interconnected through a thin cylindrical via of diameter  $d$ . The RF current through via radiates electromagnetic signal in the hybrid medium formed by the solid dielectric substrate and the air on the top. The radiated magnetic field produces induced RF current on the adjacent traces. The net current gives rise to interference voltage at the ports terminated with matched loads.

Since the via model considered here does not have pad, and the length is very small due to thin substrate, the equivalent circuit of the via is an inductance. This

# Compressive Sensing based Gender Recognition

Suparna Biswas, Jaya Sil, Sami P. Maity

**Abstract**—This paper explores an integration of compressive sensing, curvelet transform, and Principal Component Analysis to develop a robust gender recognition method from face images. Compressive measurements of face images leading to a significant reduction in feature space. Here curvelet transform has been used to represent the face images with prominent edges, curvatures, boundaries and to offer sparse representation to apply compressive measurements on detailed subband. To extract the feature vector, Principal Component Analysis is applied on the reconstructed detailed subband. Performance of the proposed method is evaluated by employing different classifiers. The proposed method efficiently handles the effect of Gaussian noise maintaining high accuracy on gender recognition. Extensive experiments on FERET database, is conducted to substantiate our claim.

**Keywords**— Gender recognition, Curvelet transform, Compressive sensing, Principal Component Analysis.

## I. Introduction

Gender recognition is an active area of research in computer vision and facing real life challenges for its commercialization. Gender recognition from face images using large set of training data has important real time applications in the fields of security, job distribution etc. It is known that men and women have discriminative facial features, which can be learned for gender recognition. In the present work we concentrate on developing an autonomous gender recognition system using face images by analyzing facial features.

Human perception involves observation of both coarse (global) and detailed (local) features of the face to identify and categorize a person. Currently different types of gender classification methods are available in the literature such as face based, gait based, hand based and many more. However, facial images are widely used for gender classification because facial images probably contain the most common biometric characteristic used by humans to make a personal recognition.

Dimensionality of features plays important role in classification accuracy because learning efficiency is affected due to presence of redundant and irrelevant features in training phase. Moreover, large number of features increases computational cost, slowing down the classification process and creates problem in real time

implementation. Therefore, appropriate feature extraction and feature selection methods together improve gender classification accuracy, which have been dealt in this paper proposing a comprehensive framework.

In 2006, Candes and Tao [1] proposed a new mathematical theory and algorithm of compressed sensing (CS) framework, which is a breakthrough of Nyquist sampling theorem. According to CS theory, the sampling frequency could be far below the Nyquist rate as long as signals are sparse and compressible in the measurement space. CS theory and sparse representation of signals allow processing with few numbers of samples and recovering it with low distortion. In this paper we present a CS theory based robust gender recognition scheme to solve the real time gender recognition problem.

Objective of this work is to extract the detail edge information utilizing curvelet transform (CT) which is more relevant to recognize the gender and also offers a sparse domain to reduce the storage space of input images. This paper actually proposes an integrated framework using CS, CT and Principal Component Analysis (PCA) for recognition of gender. PCA has been applied on reconstructed detail subband images to select important features with low dimensional space.

The paper is organized as follows: Section II presents a brief review of gender recognition method, Section III presents the scope and contributions of the proposed method. Section IV describes the proposed gender recognition method and in Section V results are discussed. Section VI concludes the paper.

## II. Literature Review

Feature extraction methods for gender recognition can be broadly classified into two categories: geometric approaches and appearance based approaches. Dimension of feature vector increases when pixel intensity is used as features resulting increase of the computational time of recognition as well. Dimension reduction technique such as PCA [2], [3] provides a representation of image in reduced dimension space. Santosa et al. [4] proposed a PCA based gender recognition method, where Support Vector Machine (SVM) is used for classification. Two-dimensional PCA (2DPCA) is an extension of PCA, used for dimension reduction of feature vector. Lu et al. proposed a 2DPCA based expression invariant gender recognition method in [5]. Gender recognition includes Linear Discriminant analysis (LDA) [6] and Independent Component Analysis (ICA) [7].

In 2002 Ojala et al. [8] introduced a new feature descriptor, Local Binary Pattern (LBP) for grayscale images. In [9] an LBP based feature extraction technique is proposed for recognition of gender. After dividing the face image into equal sized blocks, LBP is applied for multi-view gender classification. Alexandre [10] combined LBP with intensity and shape features using a multiscale fusion approach. In [11], LBP is combined with contrast information for gender classification where local contrast histograms are used as

---

Suparna Biswas  
Indian Institute of Engineering Science and Technology  
India  
Suparna\_1993@iitbbsu.co.in  
Soya Sil  
Indian Institute of Engineering Science and Technology  
India  
jsil@iitbbsu@gmail.com  
Sami P. Maity  
Indian Institute of Engineering Science and Technology  
India, samipmaity@iitbbsu.co.in

# Interference Effects of Via Interconnect in Three Layer Printed Circuit Board

Avali Ghosh, Sisir Kumar Das, and Annapurna Das

Guru Nanak Institute of Technology  
JIS Group, 157/F, Nilgunj Road, Sodepur, Kolkata-700114, India  
avalighosh@gmail.com, dean\_gnit@jisgroup.org, director\_gnit@jisgroup.org

**Abstract** — Cylindrical vias are commonly used for interconnection in multilayered Printed Circuit Board (PCB) design. The RF current through vias causes radiated interference to adjacent traces. This paper describes an analytical method of computing the radiation from cylindrical via using the electromagnetic theory. Three layer printed circuit board consisting of three traces on the top of a dielectric substrate, a middle orthogonal trace and a ground plane at the bottom, is considered. The RF voltage coupling at the terminations of the traces due to the near field radiation from the via is computed. The reactive couplings between the traces are determined from the parasitic elements using transmission line equations. The total coupling obtained from analytical method is compared with those of modeling and simulation with Ansoft HFSS software tool. The total crosstalk is also measured using an available Network Analyzer. A good agreement is found. The changes of radiated coupling with the change of position of via, trace separation and trace length are also investigated. This paper shows that the analytical method is a useful tool for predicting interference in PCB without using expensive simulation software.

**Index Terms** — Crosstalk, electromagnetic compatibility, PCB, transmission line, via, via inductance.

## I. INTRODUCTION

Analysis of reactive cross-talk between the traces in multilayer printed circuit board is described by Paul [1] using transmission line theory and results are well documented. In multilayer PCB, vias are placed to interconnect signals from one layer to another. Their locations are optimized for desired circuit operation with signal integrity and Electromagnetic Compatibility (EMC). Very costly software tools are utilized for this purpose. The effects of via interconnects are analyzed by many authors [2-12]. Pucel [2] developed an empirical formula for via inductance using image concept. Goldfarb and Pucel [3] developed empirical formula for via inductance based on measurements and numerical simulation. Cui et al. [4] described EMI problem due to via transitions through the DC power bus. Li et al.

[5] and Suntives et al. [6] have shown shielding of interference between PCB traces using an array of vias in a trace. Nam et al. [7] shown EMI mitigation in PCB using shorting vias around the signal via. Ndip et al. [8] described techniques to solve electromagnetic reliability problem due to return current paths through via by introducing layer stack up scheme. Jiang and Fan [9] has given an intrinsic via circuit model through rigorous electromagnetic analysis. Wu and Fan [10] analytically predicted crosstalk among multiple vias between infinitely large parallel planes. Pan and Fan [11] given an equivalent multi-conductor transmission line model to characterize via structures in multi-layer PCBs for signal integrity in high speed digital circuits. Isidoro-Munoz et al. [12] presented closed-form expressions for the via-pad capacitance and via-traces inductance for the performance assessment and optimization of signal integrity. None of the above publications described the analysis of radiation from via and its effects on the adjacent lines. Some results of radiation coupling from via placed in a fixed position are presented by the authors in international conferences [14,15].

In this paper the effects of via (interconnect) in a three layer PCB are described along with the reactive crosstalk between the traces. The three layer board consists of three parallel traces (Trace1, 2 and 3) on the top of a FR4 dielectric substrate (copper clad FR4 glass epoxy, S3110, CEM-1), a second layer trace (Trace 4) which is orthogonal to the top traces, and a bottom layer of ground plane as shown in Fig. 1. The single layer thickness of the substrate is  $h$  and having dielectric constant  $\epsilon_r$ . The trace 1 and trace 4 are interconnected through a thin cylindrical via of diameter  $d$ . The RF current through via radiates electromagnetic signal in the hybrid medium formed by the solid dielectric substrate and the air on the top. The radiated magnetic field produces induced RF current on the adjacent traces. The net current gives rise to interference voltage at the ports terminated with matched loads.

Since the via model considered here does not have pad, and the length is very small due to thin substrate, the equivalent circuit of the via is an inductance. This

# Analysis of PCB to find Trace Impedance by Method of Moment and Cross-talk Interference

Avali Ghosh<sup>1</sup>, Sisir Kumar Das<sup>2</sup>, Annapurna Das<sup>3</sup>

<sup>1, 2, 3</sup> ECE Department, MAKAUT, GNIT, Kolkata

**Abstract:** In this paper the impedance of PCB trace is calculated from the charge distribution on microstrip line using method of moment. The parasitic element values are computed to find the crosstalk interference in PCB. The results of theoretical analysis are obtained by using MATLAB. The crosstalk interference also found using modeling and simulation with Ansoft HFSS tool. These results are compared with the experimental results and found good agreement.

**Keywords:** Crosstalk, Multi-conductor PCB traces, Near - end crosstalk, Far - end crosstalk, Method of Moment.

## I. INTRODUCTION

Double layer printed circuit board consists of multi-conductor microstrip traces. In dense PCB designs, crosstalk interference occurs due to electromagnetic coupling between signal traces through mutual inductances and mutual capacitances. Several authors analyses coss-talk in PCB[1-10]. In this paper the line parameters such as capacitances and characteristic impedance are calculated from the charge distribution on the trace by method of moment. The parasitic element values are computed to find the crosstalk interference in PCB. The crosstalk interference also found using modeling and simulation with Ansoft HFSS tool. These results are compared with the experimental results and found good agreement.

## II. LINE IMPEDANCE USING METHOD OF MOMENT

In high-speed systems, control of the electrical characteristics of the transmission lines is crucial. The basic electrical characteristics that define a transmission line are its characteristic impedance and its propagation velocity. In this analysis the PCB traces of equal width  $w$  above a FR-4 dielectric substrate of thickness  $h$  and dielectric constant  $\epsilon_r = 4.4$  are considered above a ground plane. The line impedance of the trace can be obtained using empirical formula [11]. These formulae was derived using some assumptions and depend on trace width/substrate thickness. The traces are designed in this paper very accurately for 50 ohm using Method of Moment as described below

### A. MOM Segmentation

For surface charge distribution, the microstrip section is divided into  $N$  sections as shown in Fig. 1.

$$n = 1, 2, 3, \dots, M \text{ on the strip} \tag{1a}$$

$$n = M + 1, M + 2, M + 3, \dots, N \text{ on the ground plane} \tag{1b}$$

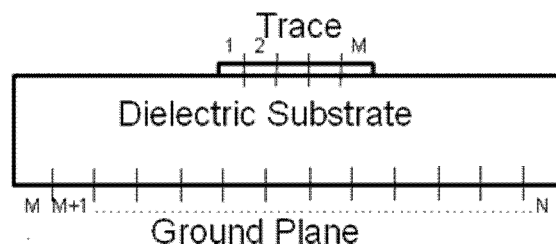


Fig. 1 Cross-sectional view of Microstrip section

Charge density  $\rho$  is constant on each segment  $\Delta S_n$

$$\rho = \sum_{n=1}^N \alpha_n f_n ; \tag{2}$$

# Minimization of Crosstalk in PCB

Avali Ghosh<sup>1</sup>, Sisir Kumar Das<sup>2</sup>, Annapurna Das<sup>3</sup>

<sup>1, 2, 3</sup>ECE Department, MAKAUT, GNIT, Kolkata

**Abstract:** This paper describes the cross-talk problems in printed circuit board design. Some models consisting of multi-conductor PCB traces above a ground plane are taken. Theoretical analysis in time and frequency domains is carried out to obtain results for near-end and far-end cross-talks by using MATLAB. These results are compared with those obtained from modeling and simulation using Ansoft HFSS-12 software and experimental results. All the results are found in good agreement. The reduction techniques of cross-talk are highlighted.

**Keywords:** Crosstalk, Multi-conductor PCB traces, near - end crosstalk, Far - end crosstalk, Micro-strip.

## I. INTRODUCTION

Crosstalk is an unwanted electromagnetic coupling from source trace to the victim trace in the printed circuit board. It occurs due to near-field / reactive field electromagnetic coupling between signal traces through mutual inductance and stray/mutual capacitance between two or more conducting traces. The cross-talk at a given terminal is calculated by the ratio of voltages between the said terminal and the input terminal, viz.,  $V_i/V_1$ , where  $i$  is the terminal at which the cross-talk is measured for input at terminal 1.

## II. CROSSTALK ANALYSIS IN FREQUENCY AND TIME DOMAIN

For crosstalk analysis a microstrip configuration having two traces with equal widths  $w$  and separated by  $s$  are placed on a lossless dielectric substrate of thickness  $h$ , is considered as shown in Fig. 1. The substrate has a dielectric constant  $\epsilon_r=4.4$  and permeability  $\mu_0$ . The ground plane and the traces are assumed to be perfectly conducting. All the traces are 50 ohm and matched terminated.

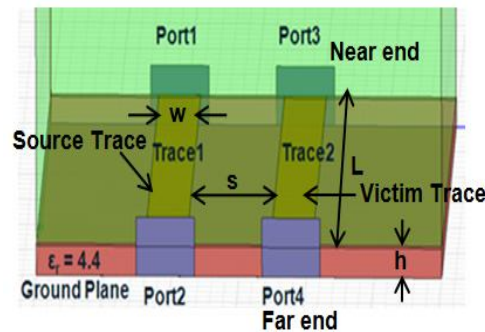


Fig. 1 PCB design describing Crosstalk

An electrically short length of PCB (i.e. line length much shorter than the minimum wavelength of interest,  $l < \lambda/10$ ), can be modeled by the lumped equivalent circuit as shown in Figure 2.

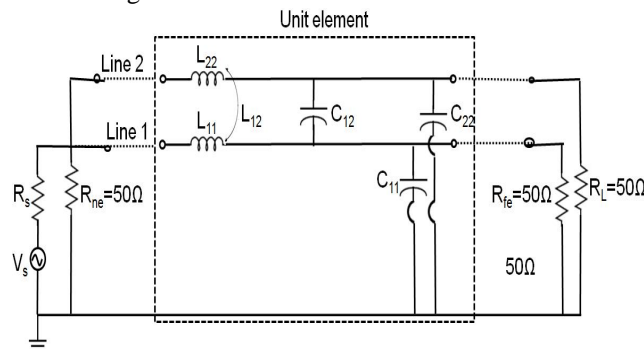


Fig. 2 Equivalent circuit of Crosstalk Model of PCB

In a homogeneous medium, if the traces or lines are weakly coupled and  $l \ll \lambda$ , the near and far end voltages are obtained from equations as [1]

# DESIGN OF A UWB ANTENNA ARRAY FOR KA BAND OPERATION

<sup>1</sup>Anurima Majumdar, <sup>2</sup>Sisir Kumar Das, <sup>3</sup>Annapurna Das

<sup>1</sup>Asst Prof, <sup>2</sup>Prof, <sup>3</sup>Prof

<sup>123</sup>Department of Electronics & Communication Engineering,  
<sup>123</sup>Guru Nanak Institute of Technology, Kolkata, India

**Abstract:** An ultra wide band circular ring patch antenna array is investigated in this paper. The initial design was a single element annular ring patch antenna fed with microstrip line on FR4 dielectric substrate with  $\epsilon_r = 4.4$  and thickness  $h=1.6$  mm. Eigen value solution for 28 GHz yields inner radius  $a=3.0$  mm and outer radius  $b= 4.05$  mm for the patch. The single element shows a bandwidth of 37.2 % at 28.5 GHz with -21dB return loss. The antenna with four connected annular rings array, fed with microstrip line, shows enhanced bandwidth of 57.57 % at 28 GHz with return loss of -23.5 dB. The array also shows multi frequency response. The designed antennae can be used in wireless communication(Abstract).

**Index Terms:** Annular ring antenna, array antenna, ultra wide bandwidth antenna, wireless communication

## I. Introduction

Printed antennas are small size, light weight, easy to install and conformal in shape. They are effectively used in wireless communications. One of the main drawbacks in microstrip antenna is narrow bandwidth. Therefore several techniques are used to increase the bandwidth. Waqas Farooq , et all [1] has reported a novel wearable antenna operating at 5 GHz where a microstrip patch is mounted on a gold base and wearable as a finger ring. By simulating it with CST Microwave studio it showed a good bandwidth of 90.3 MHz. Syed S. Jehangir and M. S. Sharawi [2] presented a semi ring slot yagi like antenna operating at 3.6 GHz. The measured bandwidth of the antenna is reported to be 374 MHz and directivity of 4.2 dB. In order to achieve higher gain, directivity and high front to back ratio (FBR), they have used a simple reflector element and achieved higher FBR. Salai Thillai Thilagam.J, et all [3], have reported an Octagonal shaped planar antenna which gave a bandwidth from 2 GHz to 10 GHz over wide multi resonant frequencies when simulated with Ansoft HFSS. A reconfigurable single slot-ring antenna using 32 PIN diode switches is proposed by Mahmoud Shirazi, et all [4] which is able to switch between S and C bands. Here the first design of a single slot ring gave a fractional bandwidth of 11.4% which was increased significantly and enhanced to 28.2% . Djelloul Aissaoui et all [5] reported a novel design of a fractal antenna for achievement of ultra Wide band response. In this paper five iterations are applied on hexagonal-cut circular antenna which is fed with a coplanar waveguide (CPW) feed. The simulation result showed a 8.6 GHz impedance bandwidth for operation ranging from 5.8 GHz to 14.4 GHz. Mohammad Shakawat Hossain,et all [6]presented a method of generation of wideband circular polarization (CP) using a stacked patch-ring microstrip antenna with a single probe feed. The proposed antenna displayed an enhanced 3dB axial ratio bandwidth of 8% and a simulated impedance bandwidth of 16%. Zhi Shen, et all [7] proposed a novel design of broadband radiation of the SIW cavity backed ring slot antenna. Experimental analysis confirmed an achievement of 12% bandwidth. Saurabh Dwivedi et all [8] reported a design technique where resonating frequency is reduced by lengthening the excited surface current path without increasing antenna length. After this an annular ring is introduced in between the symmetrical L-slotted patch and the resonance frequency is reduced by 29.91% when edge-fed or microstrip-line feed technique is used. The reported bandwidth of the final antenna is 100 MHz at 2.46 GHz. Yuanyuan Zhang [9] has investigated a centre-fed circular patch antenna with two coupled annular rings. They reported that due to the proper coupling of the two annular rings a wide band from 5.45 GHz to 7.16 GHz is achieved .In their measured result the reported bandwidth is 27.1%. A compact ring shaped monopole antenna is proposed by Rahul Singha, D. Vakula and N V S N Sarma [10] resulting in a impedance bandwidth from 6.5 GHz to 25 GHz which covers the entire UWB. Ashish Singh, et all [11] carried out a theoretical analysis of a slots and notches loaded microstrip patch antenna to achieve dual band operations. The bandwidth of the proposed antenna at  $TM_{01}$  mode is 3.42 % , at  $TM_{02}$  mode it is 3.81 % and for  $TM_{03}$  mode it is 4.80 % .

In this paper a microstrip annular ring and its array are designed as shown in Fig.1. The annular ring is designed at 28 GHz for the radiation mode of excitation  $TM_{120}$  .The antenna is fed with a 50 ohm microstrip line. Then the number of elements is increased to four and placed at suitable locations to form an array. Power is divided into the four elements through 50 ohm lines of different lengths. The design is characterised using Ansoft HFSS software tools for amplitude and phase distribution of power for enhanced bandwidth and desired radiation pattern. It is seen that the second configuration with four ring arrays gave increased bandwidth and also multi frequency response.

## II. Simulation and Design of the Antenna Structure

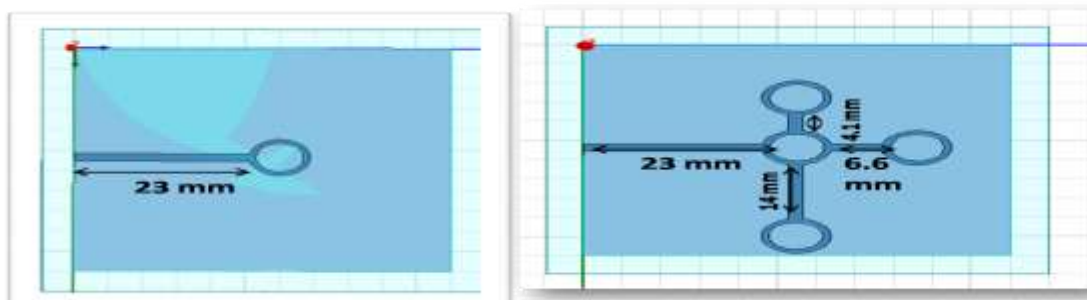


Fig 1. (a) A single element annular rings array (b) A four element annular rings array

# A Wideband Multiband CPW Fed Wineglass Shaped Patch Antenna with Tuning Stub for 4G Wireless Communication Application

Anurima Majumdar<sup>1</sup>, Sisir Kumar Das<sup>2</sup>, Annapurna Das<sup>3</sup>

<sup>1, 2, 3</sup>Guru Nanak Institute of Technology, India

**Abstract:** A novel design of a wineglass shaped patch antenna with tuning stub is inspected in this paper. FR4 epoxy with  $\epsilon_r=4.4$  is used as dielectric substrate with height 1.6 mm. The antenna resonates at design frequency 3.4 GHz and gives multifrequency response at 3.1 GHz, 1 GHz and 4.4 GHz. The impedance bandwidth below -10dB return loss is 19.35 % at 3.4 GHz with return loss -25 dB. The analysis of the antenna is done using HFSS simulation tool.

**Keywords:** Wideband, multiband, CPW feed, tuning stub, wireless communication

## I. INTRODUCTION

Microstrip Antennas are very useful and efficient different radio communication systems starting from wireless communication to satellite communication. Different techniques has been investigated to improve the performance parameters of the patch antennas like getting multi frequency multi band response or higher impedance bandwidth response, better gain. Yao Chen, Longfang Ye, Jianliang Zhuo, Yanhui Liu, Liang Zhang, Miao Zhang, and Qing Huo Liu reported a reconfigurable circular patch antenna with an arc shaped slot loaded in the ground plane in their paper[1]. They have used 5 PIN diodes for matching. By changing the length of the arc slot six frequency band reconfigurations were achieved. Nozomu Ishii, Kiyohiko Itoh has discussed the mechanism of tuning stub for a circular polarised annular microstrip antenna in their paper [2]. D. D. Krishna, M. Gopikrishna, C. K. Anandan P. Mohanan and K. Vasudevan has discussed[3] a compact dual frequency slotted circular microstrip patch antenna with a dielectric superstrate which improves the bandwidth and lowers the resonant frequencies. The size reduction is reported to be 60 % along with better antenna performance. Surendra K roy and Lalan Jha has discussed the effect of the length modification of tuning stub on resonant frequency in their paper[4]. In this paper a CPW fed wine glass shaped patch antenna with tuning stub is investigated for multiband operation and bandwidth enhancement.

## II. DESIGN SIMULATION AND RESULTS

A wine glass shaped patch antenna is designed using HFSS tool showed in Fig.1. Here the co planar waveguide fed technique is used for feeding. The design frequency is at 2.4 GHz. A tuning stub is used for better impedance matching. FR4 epoxy with  $\epsilon_r = 4.4$  is used as dielectric substrate with height 1.6 mm. The dimension of the dielectric substrate is 55mm X 55mm. The ground plane is introduced with a circular slot of radius 17mm. All the design parameters are given in details in the below mentioned table I.

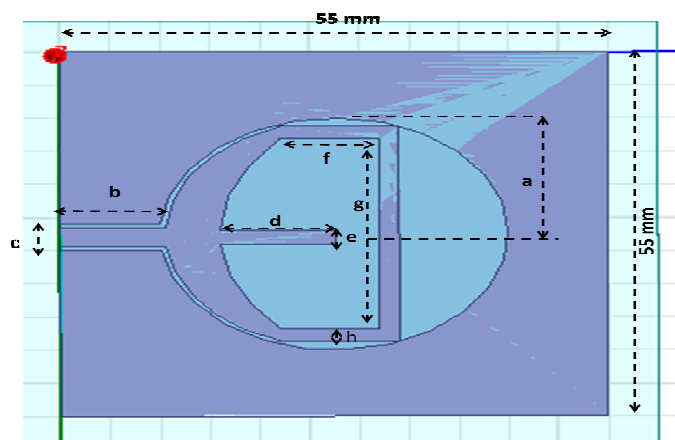


Fig 1 : A CPW fed wine glass shaped patch antenna with tuning stub



# Cross layer optimization for outage minimizing routing in cognitive radio ad hoc networks with primary users' outage protection



Surajit Basak, Tamaghna Acharya\*

Department of Electronics & Telecommunication Engineering, Indian Institute of Engineering Science and Technology, Shibpur 711103, India

## ARTICLE INFO

### Keywords:

Cognitive radio ad hoc networks  
Cross-layer approach  
Distributed routing  
End-to-end outage probability

## ABSTRACT

Path selection to minimize end-to-end (e2e) outage experience of cognitive users (CUs) in a given communication session is one of the key challenges in multi-hop cognitive radio ad hoc networks, where each CU node experiences a unique spatio-temporal variation of spectrum access opportunity. We study the problem under the constraint of probabilistic interference to primary receivers, in contrast to the popular trend of considering detection probability of primary user (PU) transmissions. This is formulated as a joint transmit power control, spectrum assignment and routing problem and a constrained optimization framework are presented for it. Further, using a standard technique for solving the convex optimization problem, a closed form expression for the transmission power of source as well as relay nodes is derived. Based on this, a centralized solution is proposed for optimal spectrum assignment and route selection. In addition, due to the prohibitive complexity of the optimal solution, a low complexity spectrum aware-outage minimizing opportunistic routing (SA-OMOR) solution is presented, along with its possible distributed implementation. Simulation results are used to validate our analytical results as well as the performance comparison between the proposed SA-OMOR scheme and the optimal one.

## 1. Introduction

A cognitive radio ad-hoc network (CRAHN) (Akyildiz et al., 2009), where each user, also referred as cognitive user (CU), is equipped with a cognitive radio (CR) transceiver based network interface card, offers a self organized, fast deployable, multi-hop and scalable wireless network architecture without the help of any dedicated physical infrastructure. Possible deployments of CRAHNs include smart grids (Khan et al., 2016), IoT for smart cities (Afzal and Zaidi et al., 2015), disaster management (Onem et al., 2013), military operations (Younis and Kant et al., 2010), etc. For successful deployment of CRAHNs in many of the above applications, solving routing problem is imperative. However, routing in CRAHNs is a highly daunting task since the existing routing challenges of wireless ad hoc networks (WANETs), inherited by such networks, get coupled with the uncertainty in the underlying spectrum availability, constrained spectrum access privileges and imperfect spectrum sensing (SS). Hence designing a routing metric, exploiting novel interactions between the routing and the spectrum management functionalities, is of paramount importance in any efficient routing protocol. A comprehensive survey of the available routing metrics may be found in Singh and Moh (2016). As noted in Singh and Moh (2016), both single path and multi-path routing metrics are designed based on some

traditional performance metrics like delay, hop count, power consumption, as well as some new performance criteria unique to CRAHNs like spectrum availability, route stability. Cluster based collaborative multi-hop routing has received great attention to improving network performance in CR network. In Jiang et al. (2015b), the authors proposed a collaborative multi-hop routing strategy to maximize the network throughput. Jiang et al. (2016b) proposed a joint power control, spectrum assignment, and cluster based collaborative multi-hop routing algorithm to improve spectrum efficiency in CR network.

For the above reasons, we are motivated to further investigate the routing problem in CRAHNs. Our goal is to support reliable communication of delay sensitive traffic over a multi-hop wireless fading link in a CRAHN which could operate without any dedicated spectrum for communication.

### 1.1. Related works

In Jayasinghe and Rajatheva (2010), transmit power control problem is addressed aiming to minimize the end-to-end (e2e) outage probability in a relay assisted CR network with underlay mode (Goldsmith et al., 2009), of operation. A similar problem is dealt in Yu et al. (2012), considering a joint SS and data transmission

\* Corresponding author.

E-mail addresses: [surajit.basak2007@gmail.com](mailto:surajit.basak2007@gmail.com) (S. Basak), [t\\_acharya@telecom.iests.ac.in](mailto:t_acharya@telecom.iests.ac.in) (T. Acharya).



# On prediction error compressive sensing image reconstruction for face recognition ☆

Suparna Biswas <sup>a</sup>✉, Jaya Sil <sup>a</sup>✉, Santi.P. Maity <sup>b</sup>

Show more ▼

+ Add to Mendeley  Share  Cite

<https://doi.org/10.1016/j.compeleceng.2017.11.009>

[Get rights and content](#)

## Abstract



Contents lists available at ScienceDirect

Computers and Electrical Engineering

journal homepage: [www.elsevier.com/locate/compeleceng](http://www.elsevier.com/locate/compeleceng)

## On prediction error compressive sensing image reconstruction for face recognition<sup>☆</sup>

Suparna Biswas<sup>A,\*</sup>, Jaya Sil<sup>A</sup>, Santi.P. Maity<sup>B</sup><sup>A</sup>Department of CST, Indian Institute of Engineering Science & Technology, Shibpur-711021, India<sup>B</sup>Department of IT, Indian Institute of Engineering Science & Technology, Shibpur-711021, India

### ARTICLE INFO

#### Article history:

Received 21 March 2017

Revised 25 October 2017

Accepted 7 November 2017

Available online xxx

#### Keywords:

Autorecoder

Compressive sensing

Face recognition

Image predictors

Image reconstruction

### ABSTRACT

This paper explores the scope of spatial domain sparse representation for the application to develop a fast and robust remote end face recognition (FR) scheme in the framework of compressive sensing (CS). At the source end, error images as the difference between the original and the predicted images, are obtained using the different predictors that offer compressive measurements. Sub-sample measurements of the sparse error image and part of the original image are then transmitted. At the destination end, the test image is obtained from its partial information and CS reconstructed error image. Principal Component Analysis is used to extract the important features from the reconstructed image followed by FR. Performance of the proposed method is studied using collaborative representation based classifier with regularized least square method, applied on two databases, AR and ORL and an accuracy of 93.99% for the former and 91.5% for the latter is observed.

© 2017 Elsevier Ltd. All rights reserved.

### 1. Introduction

Face recognition (FR) offers a cost effective means for identification of individuals using low cost camera and at the same time without using any prior knowledge. Some times FR can be accomplished at lower sampling rate, for example, surveillance in crowded places like railway station, airport and shopping mall that need fast sensing of images in order to recognize the persons with less time and at low space complexity. The other application may be FR at remote end through bandwidth efficient transmission of samples using compressed sensing or compressive sampling (CS) a relatively new technique that appears as a potential solution to sub-sample signal reconstruction.

Literature on FR is quite rich, methods include principal component analysis (PCA), and its various variants, namely symmetrical PCA, two-dimensional PCA [1], weighted modular PCA, various types of linear discriminant analysis (LDA), namely direct-weighted LDA, generalized LDA using singular value decomposition (SVD) [2], local binary pattern (LBP) [3], histogram of oriented gradients (HOG) [4] etc for feature extraction. Researchers apply different types of classifiers, like K-nearest neighbor (KNN) [3], support vector machine (SVM) [5] etc on the feature vectors for FR. Recently sparse representation based classifier (SRC), collaborative representation based classification with regularized least square (CRC\_RLS) [6] and CS in kernel based SRC [7] are also used in FR at reduced feature space.

<sup>☆</sup> Review processed and recommended for publication to the Editor-in-Chief by Area Editor Dr. E. Cabal-Neyez.

\* Corresponding author.



Copyright © 2017 American Scientific Publishers  
All rights reserved  
Printed in the United States of America

# A Compressive Sensing Based Robust Face Recognition Method

Suparna Biswas

Gurunank Institute of Technology, 700114, India

\*Suparna\_b80@yahoo.co.in

**Abstract:** In this paper an integrated face recognition method has been proposed to recognize the face images. This integrated framework combines the compressive sensing (CS) and Local Binary Pattern (LBP). The image is at first divided into small blocks and local binary pattern is generated corresponding to each block. Features are extracted from the LBP transformed image using blockwise histograms with variable no of bins. For classification we use compressive sensing based sparse representation classification (SRC). To study the robustness of our method, the classifier is studied on clean and occluded images. The experimental results give promising performance of the proposed face recognition method on JAFFE and ORL database

**Keywords:** Face recognition; compressive sensing; local binary patterns.

## 1 INTRODUCTION

Face recognition is a challenging problem in the field of image analysis and computer vision. Many researchers in face recognition have been dealing with the challenge of pose variations, illumination differences, facial expressions and occlusions. Efficient recognition algorithms can reduce the effect of noise and other challenges. Automatic face recognition accuracy involves two important steps: first one is facial feature extraction techniques and second is classifier design.

A number of methods have been developed for extracting features from the face images. Recently developed MGA tools are widely used in feature extraction, such as curvelet [1, 2], bandlet and contourlet [3, 4] etc. N. G. Chitaliya and A. I. Trivedi proposed a contourlet and Principal Component Analysis (PCA) based face recognition method in [5]. Their results show that the proposed method performs better than the method based on

wavelet transforms. Wang et al. [6] have developed an efficient face recognition method based on contourlet and SVM. Huang et al. [7] built a face recognition method based on illumination invariant features in contourlet domain showing results which are effective and competitive with respect to other methods.

Classifier design is another important task in case of face recognition problem. Recently Compressive sensing based classifier named as sparse representation classifier (SRC) is widely used in face recognition. Actually Compressive sampling or compressive sensing technique presents a new method to capture and represent compressible signals at a rate significantly below the Nyquist rate. This CS based SRC classifier shows better performance than the other classifiers. At first Wright et al. [8] proposed the SRC classifier to solve the face recognition problem. In this work

# Link Layer Capacity of MIMO Ad Hoc Network with Noise Environment

Soma Manna<sup>1</sup> Dr. Arun Kumar Mondal<sup>2</sup>

<sup>1,2</sup>Department of Electronics and Communication Engineering

<sup>1,2</sup>Gurunanak Institute of Technology, Kolkata, India

**Abstract**— MIMO Ad Hoc Networks are expected to provide broadband wireless service parallel to wired counterpart and may be replaced for emergency services. MIMO holds the significant promise to maximize the resource uses. In this paper, the channel capacity analysis is made based on a model MIMO Ad Hoc network assuming that each link occupies a geometric area that characterizes the amount of spatial resources occupied by a link. The amount of spatial resource of each link is considered with the interference effects that inflicts on other links. The link layer capacity is investigated here considering the noise effect for the above MIMO Ad Hoc Network employed in the noisy environment. The cumulative distribution function of signal to noise ratio with interference effect is calculated first and then throughput of the communication link is derived. Finally simulated results are shown considering different number of nodes. This result helps to find out number of active links and data rates within an area.

**Key words:** MIMO, Link Layer Capacity, Co-Channel

## I. INTRODUCTION

A mobile ad hoc network (MENET) represents a system of wireless mobile nodes that can freely and dynamically self-organize into network topologies. It is basically peer-to-peer network of hosts connected by wireless links.[1,2] It has been observed that the MIMO technologies help to boost the significant advances and lead to potential break through towards robust Ad Hoc Network design. Wireless data rate for multiple-input-multiple-output (MIMO) systems with multiple antennas at both transmitter and receiver obey the following fundamental theoretical limit:

$$C = M \cdot \log(1 + \frac{P}{N}) \quad (1)$$

Where  $M = \min \{M_t, M_r\}$ , and  $M_t, M_r$  are the number of antennas at transmitter and receiver, respectively, provided that an improvement of the rate factor by  $M$ [3].

MIMO system uses multiple transmitters and receivers to create additional paths or radio channels for the wireless transmission where each path operates independently as the paths are orthogonal in communication channels and the receiver recognizes this [4]. This requires a high-signal-to-noise ratio which uses sophisticated algorithms to separate the paths which overlap in time and frequency. The key benefit of MIMO is that it offers significant increases in data throughput and link range without additional bandwidth or transmit power [5]. It achieves this by higher spectral efficiency (more bits per second per Hertz of bandwidth)[6] and link reliability or diversity (reduced fade)[7]. For noise free channel, the average amount of information received would be  $H(X)$  bits per symbol, when interference and noise are added to the receiving signal, then amount of information received by the receiver is the ergodic mutual information between the channel input and output which can be expressed in terms of two conditional entropies:  $E(H(y_k))$  known as the self-entropy of the channel without any knowledge about the received signal  $y_k$  and  $E(H(y_k/x_k))$  known as the

conditional entropy of the channel with the knowledge of a particular received signal  $y_k$ . The mutual information  $I(X; Y)$  between the channel input and output is the amount of uncertainty obtained by difference between the above two entropies and is given as,

$$\begin{aligned} I(X; Y) &= E(H(y_k) - H(y_k/x_k)) \\ &= E(H(y_k) - H(n)) \\ &= E(\log \det(I + \eta H R H^H + \sigma^2 I)) \end{aligned} \quad (2)$$

Here the element  $H$  is a  $N_T \times N_R$  matrix that has a complex Gaussian distribution.  $\eta(k)$  is the  $N \times 1$  additive white Gaussian noise vector with zero mean and matrix covariance  $C_w$ .

If the set of signals are independent and excited by different transmitters and detected by receiver then the element  $H$  will be independent as well. It is observed that if these two conditions are satisfied, the maximum mutual information will be obtain and that will be MIMO channel for a given transmitter power. The ergodic capacity for channel matrix  $H$  is given as:

$$C = E_H \left\{ \log_2 \det \left( I_{N_R} + \frac{P}{P_N N_T} H H^* \right) \right\} \quad (3)$$

We have considered the large network so that homogeneous channel and interference conditions occurred. Under this condition throughput of each link is same and summation of that is equivalent to channel capacity. We assume that the network is quasi stationary and outage capacity of the channel is

$$C = \log_2 \left\{ \det \left( I + \frac{P}{P_N N_T} H H^* \right) \right\}$$

For  $K$  burst or hops.

The random channel matrix  $H_k$  is varying from one burst to the next,  $H_k$  will itself vary accordingly.

In this paper we should find out the link failure due to interference and also interference cancellation between MIMO links.

This gives us the information about the failure of the transmission as well as success or throughput of the probability of the output of the network.

Finally the link layer capacity is calculated and simulated to get the results.

## II. SYSTEM MODEL AND CHANNEL CAPACITY

The fig1 shows the system model of mobile Ad Hoc Networks with multiple antennas. The mathematical analysis of this model is done with some assumptions. We assumed here that the MIMO nodes are uniformly distributed within the network area, and assume that each link between the transmitting and receiving antenna has same statistical characteristics. The topology of the network changes dynamically and distributed over the nodes forming the networks. Here all transmitting nodes are connected to the receiving nodes using mobile links. Let us consider that the node  $R$  is the receiving node where the other nodes are transmitting nodes without loss of generality the link  $H_R$  is



## Enhancement of TCP Performance over MANET

Soma Manna<sup>1</sup>, Arun Kumar Mondal<sup>2</sup>, Pratiti Roy<sup>3</sup>

<sup>1</sup>Assistant Professor, Dept. of ECE, GNIT, Sodepur, Kolkata - 700114

<sup>2</sup>Professor, Dept. of ECE, GNIT, Sodepur, Kolkata – 700114

<sup>3</sup>Student, Dept. of ECE, GNIT, Sodepur, Kolkata - 700114

\*\*\*

**Abstract** - Mobile ad hoc networks (MANET) plays an important role in today's communication. The Ad hoc networks are a new wireless networking paradigm for mobile hosts. To facilitate communication within the network a routing protocol is used to discover routes between nodes. The goal of the routing protocol is to have an efficient route establishment between a pair of nodes, so that messages can be delivered in a timely manner. Bandwidth and power constraints are the important factors to be considered in current wireless network because multi-hop ad-hoc wireless relies on each node in the network to act as a router and packet forwarder. TCP is used in communication between different applications programmers like file transfer, database management etc. in different system. In this paper we have discussed the existing TCP/IP protocol and some existing extension of this protocol TCP-F, TCP-BUS, ACTP and internet control message protocol. Finally we have given some simulated result using OPNET to find the performance of the throughput using the TCP model.

**Key Words:** MANETs, TCP, ATCP, Delay, Throughput

### 1. INTRODUCTION

Like traditional mobile wireless networks, Ad hoc networks do not rely on any fixed infrastructure. It represents complex distributed system that comprises wireless mobile nodes that can freely and dynamically self-organize into arbitrary and temporary, "ad-hoc" network topologies, allowing people and devices to seamlessly interconnect in areas with no pre-existing communication infrastructure. These nodes can be arbitrarily located and are free to move randomly at a given time, thus allowing network topology and interconnections between nodes to change rapidly and unpredictably [1, 2]. The transport layer is responsible for end-to-end connection establishment, end-to-end data packet delivery, congestion control, and flow control [3, 4]. The real time protocol RTP is a genetic real time transport protocol used in conjunction with UDP. Real time transport control protocol (RTCP) is a protocol used to provide feedback on bandwidth, congestion, and delay to RTP. TCP is a reliable, end to end, connection-oriented transport layer protocol. A comparison of UDP and TCP protocol packet format are shown.

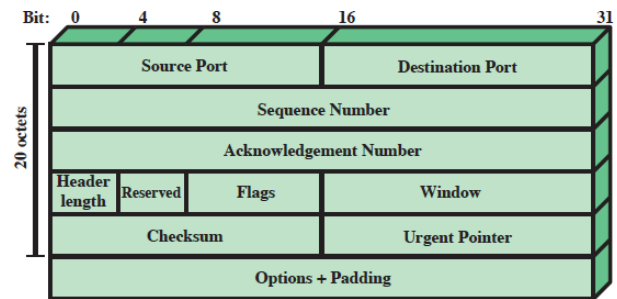


Fig1. TCP header

Wireless systems operate with the aid of a centralised supporting structure such as an access point. This access In this paper we design a protocol that has the following characteristics. *Improve TCP Performance for Connections set up in ad hoc Wireless Networks.* TCP performance is affected by the problems of high BER and disconnections due to route precomputation or partition. In each of these cases, the TCP sender mistakenly invokes congestion control [5]. The appropriate behaviour in these cases ought to be the following.

*High BER:* Simply retransmit lost packets without shrinking the congestion window.

*Delays due to Route re-computation:* Sender should stop transmitting and resume when a new route has been found.

*Maintain End-to-End TCP Semantics.* We believe that it is critical to maintain end-to-end TCP semantics in order to ensure that applications do not crash.

ATCP treats loss due to packet loss and loss due to congestion. ATCP ensures that the congestion window is recomputed after every new route re-computation. In TCP-F upon receiving the RFN, the source suspends all the packet transmissions and freezes its state, including the Retransmission time out Interval and the congestion window. Eventually the intermediate node that has previously forwarded the RFN learns of a new route to the destination. In TCP-BUS the message is propagated to the source and stops transmission, after receiving an explicit route disconnection message (ERDN) Packet transmission is resumes after a partial path has been re-established [6]. In the subsequent section we have developed a system model



# Outage Capacity of MIMO Mobile Ad Hoc Network

Soma Manna<sup>1</sup>, Arun Kumar Mondal<sup>2</sup>

<sup>1</sup>Assistant Professor, Dept. of ECE, GNIT, Sodepur, Kolkata - 700114

<sup>2</sup>Professor, Dept. of ECE, GNIT, Sodepur, Kolkata - 700114

\*\*\*

**Abstract** - With the fast progress of wireless communication and its growing application in different areas, it is important to develop technologies to enable more efficient secure communication. Mobile Ad hoc, an infrastructure less communication, is an emerging area for anytime and anywhere communication. It is very challenging to coordinate node transmission in mobile ad hoc network for secure communication. MIMO holds the significant potential to maximize the resource uses. In this paper, the outage capacity analysis is made based on a model MIMO Ad Hoc network. We assume that each link occupies a geometric area that characterizes the amount of spatial resources occupied by a link. The amount of spatial resource of each link is measured with the interference effects that impose on other links. Here we also investigated the outage capacity considering the noise effect for the above MIMO Ad Hoc Network working in the noisy environment. The probability of the active link with interference effect is calculated first and then the outage throughput capacity is derived. Finally simulated results helps to find out number of active links and data rates within an area.

**Key Words:** Mobile Ad Hoc Network, MIMO, link layer capacity, co-channel interference.

## 1. INTRODUCTION

Wireless Ad hoc networks are integral part of the new generation information exchanges infrastructure. These are basically peer-to-peer network of hosts that have no central administration or fixed communication infrastructure nor any base station[1,2]. The MIMO based Mobile Ad hoc network takes the advantages of meshed topology of the ad hoc network to maximize the data rate supporting different transmission priorities, reducing transmission delay and ensuring fair transmission among nodes. This integrated network improves the data rates and it uses IEEE 802.11n standard providing higher spectral efficiency such as high throughput to improve system performance than that of ordinary wireless systems. To achieve the performance analysis of the MIMO communication system, the channel performance

like channel characteristic, mutual information are the basic parameters to represent the mathematical modeling of channel capacity and mutual information of the MIMO ad hoc network. Wireless data rate for MIMO systems with multiple numbers of antennas at both transmitter and receiver follow the following fundamental theoretical limit:

$$C = M * B * \log(1 + SNR) \tag{1}$$

To achieve the performance analysis of the channel we have modeled the ad hoc network, mathematical representation of channel parameters (channel capacity, mutual information) with different channel state information. The availability of multiple antennas at the transmitter and receiver end improve the data rates by a factor of M times where  $M = \min\{N_T, N_R\}$ ;  $N_T$  and  $N_R$  are the number of transmitting and receiving antennas[3,4]. By using multiple antennas MIMO Ad hoc network increases channel capacity [5,6]. We can see the nodes in transmitter and receiver from NxM MIMO channel. We invoke Telatar' landmark MIMO capacity theorem.

$$C_{N,M} = E_{\lambda}\{R \log_2(1 + \frac{\lambda}{N} \rho)\} \tag{2}$$

Here  $R = \min(M, N)$ ;  $\rho = S/N$  represent the single tone noise ratio.  $\lambda$  is the unordered eigenvalue of associated Wishart matrix W.

## 2. SYSTEM MODEL AND CHANNEL CAPACITY

The fig1 shows the system model of mobile Ad Hoc Networks where mathematical analysis of this model is done with some assumptions. Here the MIMO nodes are uniformly distributed with in the network and each link between the transmitting and receiving antenna has same statistical characteristics. Here using mobile links all transmitting nodes are connected to the receiving nodes. Let us consider that the node M is the receiving node where the other nodes are transmitting nodes and the link  $H_R$  is receiving the signal and other link are transmitting signal and resulting the co-channel interference on link  $H_R$ . The data received by the receiving link is the superposition of the desired signal interference and noise which is given as follows.



# Multifrequency Microstrip Antenna for Mobile Communication

Antara Ghosal<sup>1</sup>, Poulomi Nath<sup>2</sup>, Sisir Kumar Das<sup>3</sup>  
 Assistant Professor<sup>1</sup>, PG Scholar<sup>2</sup>, Dean-Research & Administration<sup>3</sup>  
 Department of Electronics and Communication Engineering  
 Guru Nanak Institute of Technology, Kolkata, India

**Abstract:**

This paper describes the analysis and design of a class of slotted rectangular microstrip antennas for multi frequency operations. At first slots are cut to tune the patch at suitable dual frequency and then more slots are introduced to obtain multi frequency operations. The simulation and modelling of these configurations have been done using Ansoft HFSS software. The resonant frequencies and dimensions are computed from the cavity model of rectangular patch. The parameters of antenna such as return loss, VSWR, radiation patterns and gain have been found and design is optimized for best results. The results are experimentally verified and the results are found in good agreement with those of theory.

**Keywords:** Microstrip Antenna, Coaxial feed, slotted rectangular microstrip patch antenna, multiband antenna

## I. INTRODUCTION

Very recently in mobile communication system multi frequency patch antenna are rapidly dominating mobile phone handsets which are capable of operating at multi frequency for different mobile network service providers at different countries (900, 1800, 1900, 2400 MHz).

L-shaped structure as described by K.L. Wong [4], have a shorting plate at a corner, the result of which, however has not been described by him.

This paper begins with the design of an L-shaped patch antenna which operates at dual frequency. However, by introducing more number of slots on this L-shaped patch antenna it was found that the single antenna started operating at multiple frequencies.

Ansoft HFSS software is used for analytical modelling and simulation.

## II. ANALYSIS OF SLOTTED RECTANGULAR MICRO STRIP ANTENNAS

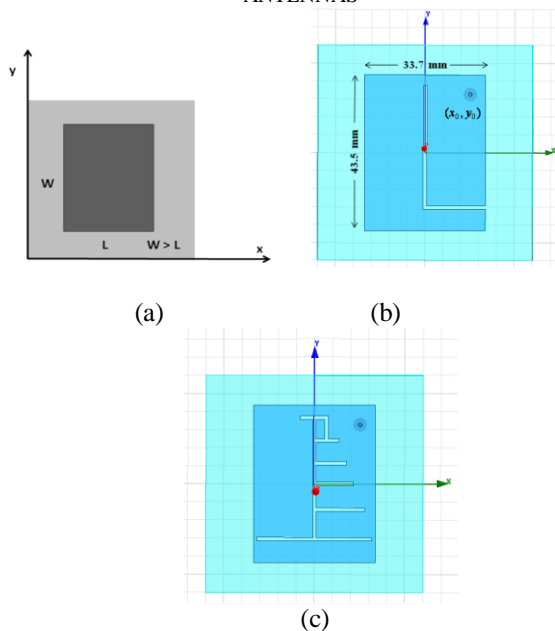


**Fig.1 Rectangular Patch**  
 (a. Plane rectangular patch b. L-shape patch  
 c. slotted rectangular patch)

The top view of a rectangular patch and a slotted rectangular patch are shown in Fig.1. Fundamental resonant frequency is determined using cavity model [1-3]. The designed parameters are: substrate  $\epsilon_r = 4.4$ , and thickness  $h = 1.6$  mm;  $f = 2.4$  GHz. Since  $W \gg h$ , effect of fringing field in mixed dielectric media, air and the substrate, replaces  $\epsilon_r$  by an effective parameter  $\epsilon_{reff}$  along length  $L$  and width  $W$ , given by

$$\epsilon_{reff}(L) = \frac{\epsilon_r + 1}{2} + \frac{\epsilon_r - 1}{2} (1 + 12h/L)^{-1/2} \quad (1)$$

$$\epsilon_{reff}(W) = \frac{\epsilon_r + 1}{2} + \frac{\epsilon_r - 1}{2} (1 + 12h/W)^{-1/2} \quad (2)$$

respectively.  $\epsilon_{reff}$  vs normalized patch dimension/h is plotted to find  $\epsilon_{reff}$  for a given dimension and is shown in Fig.2. Since  $W \gg h$ , it can be selected without considering fringing from the following:

$$W = \frac{c}{2f_r} \sqrt{\frac{2}{\epsilon_r + 1}} \quad (3)$$

Here  $c$  = velocity of light in free space

Because of the fringing effects, effective electrical length of the patch of the microstrip antenna extends on each end by a distance  $\Delta L$ , which is a function of the effective dielectric constant and the width-to-height ratio ( $W/h$ ). An approximate relation for the normalized extension of the length in one side is [1]

$$\frac{\Delta L}{h} = 0.412 \frac{(\epsilon_{reff} + 0.3) \left( \frac{W}{h} + 0.264 \right)}{(\epsilon_{reff} - 0.258) \left( \frac{W}{h} + 0.8 \right)} \quad (4)$$

The patch is excited from the ground plane using a co-axial probe at  $(x, y)$ . The fundamental resonant mode of a plane rectangular patch in the direction of excitation ( $z$ ) is  $TM_{010}$  when  $W = \lambda/2 > L$ .

# Dual Band Microstrip Antenna for Mobile Hand Set

Antara Ghosal<sup>1</sup>, Anurima Majumdar<sup>2</sup>, Sisir Kumar Das<sup>3</sup> and Annapurna Das<sup>4</sup>

Assistant Professor, Electronics & Communication Engineering, Guru Nanak Institute of Technology, Kolkata, India <sup>1,2</sup>

Dean – Research & Administration, Guru Nanak Institute of Technology, Kolkata, India <sup>3</sup>

Director, Guru Nanak Institute of Technology, Kolkata, India <sup>4</sup>

**Abstract:** This paper describes the analysis and design of a class of slotted rectangular microstrip antennas for dual band operations. Slots are cut to tune the patch at suitable dual frequency operations. The simulation and modeling of these configurations have been done using Ansoft HFSS software. The resonant frequencies and dimensions are computed from the cavity model of rectangular patch. The parameters of antenna such as return loss, VSWR, radiation patterns and gain have been found and design is optimized for best results. The results are experimentally verified and the results are found in good agreement with those of theory.

**Keywords:** Coaxial feed, slotted rectangular microstrip patch antenna, dual band antenna.

## I. INTRODUCTION

Demand of multi frequency patch antenna has been dramatically increased for mobile phone handsets which are capable of operating at multi frequency for different mobile networks at different countries (900, 1800, 1900, 2400 MHz). Several authors are described different structures for multifrequency operations [4-7]. K.L. Wong [4] described L-shape structure with shorting plate at a corner. However, he has not described the results. This paper will provide design guidance of a single antenna operable at dual frequencies by suitably cutting slot on rectangular patch without any shorting plate with ground. Ansoft HFSS software is used for analytical modelling and simulation and experimental verification of results are made using network analyser.

## II. ANALYSIS OF SLOTTED RECTANGULAR MICRO STRIP ANTENNAS

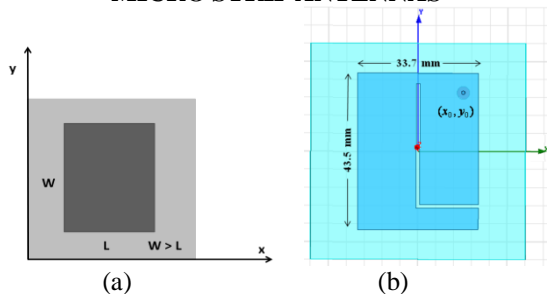


Fig.1 Rectangular Patch  
(a. Plane rectangular patch b. slotted patch)

The top view of a rectangular patch and a slotted rectangular patch are shown in Fig.1. Fundamental resonant frequency is determined using cavity model [1-3]. The designed parameters are: substrate  $\epsilon_r = 4.4$ , and thickness  $h=1.6$  mm;  $f=2.4$ GHz. Since  $W \gg h$ , effect of fringing field in mixed dielectric media, air and the

substrate, replaces  $\epsilon_r$  by an effective parameter  $\epsilon_{reff}$  along length L and width W, given by

$$\epsilon_{reff}(L) = \frac{\epsilon_r + 1}{2} + \frac{\epsilon_r - 1}{2} (1 + 12h/L)^{-1/2} \quad (1)$$

$$\epsilon_{reff}(W) = \frac{\epsilon_r + 1}{2} + \frac{\epsilon_r - 1}{2} (1 + 12h/W)^{-1/2} \quad (2)$$

respectively.  $\epsilon_{reff}$  vs normalized patch dimension/h is

plotted to find  $\epsilon_{reff}$  for a given dimension and is shown in Fig.2. Since  $W \gg h$ , it can be selected without considering fringing from the following:

$$W = \frac{c}{2f_r} \sqrt{\frac{2}{\epsilon_r + 1}} \quad (3)$$

Here  $c$ =velocity of light in free space. Since  $W \geq L$  the  $\epsilon_{reff}$  is calculated from (2) or from Fig.2. For  $h=1.6$ mm, it is found  $\epsilon_{reff} = 4.09$ .

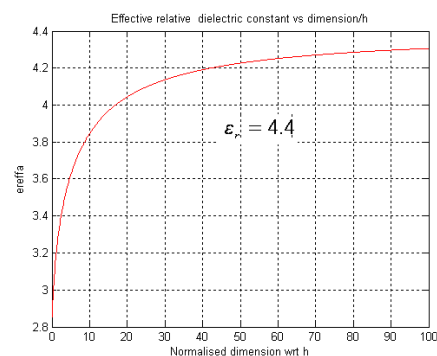


Fig.2  $\epsilon_{reff}$  vs patch dimension/h

Because of the fringing effects, effective electrical length of the patch of the microstrip antenna extends on each end

# Design and Analysis of a tuned circular patch antenna for satellite communication application in C band

Anurima Majumdar<sup>1</sup>, Antara Ghosal<sup>2</sup>, Sisir k Das<sup>3</sup>, Annapurna Das<sup>4</sup>

Assistant Professor, Electronics & Communication Engineering, Guru Nanak Institute of Technology, Kolkata, India <sup>1,2</sup>

Dean – Research & Administration, Guru Nanak Institute of Technology, Kolkata, India <sup>3</sup>

Director, Guru Nanak Institute of Technology, Kolkata, India <sup>4</sup>

**Abstract:** In this paper a novel design approach of a probe feed circular microstrip patch antenna with four tuning arms on the radiation element for the dual-frequency operation is proposed. The cavity model is used for the parameter computation of the antenna. The circular antenna resonates at 4 GHz and 5.8 GHz which enables it to operate in standard C band which is used by communication satellites. TM<sub>110</sub> is the dominant mode for this proposed antenna. The designed antenna provides 11 % bandwidth at 5.8 GHz (200 MHz) and the S[1 1] value is -42 dB whereas it provides 5.75 % bandwidth at 4 GHz (700 MHz) and the S[1 1] value is -16 dB. The absolute values of VSWR at 4 GHz is reported as 1.06 and at 5.8 GHz is 0.08. A further modification is done on the proposed patch and a comparison of the designs are reported.

**Keywords:** Coaxial feed , circular microstrip patch antenna, C band , tuning arms, satellite communication.

## I. INTRODUCTION

With the rapid advancement in the field of Satellite communications and wireless communication the demand of Microstrip patch antenna is also increased due to its compact , low profile structure. K.L Wong has discussed different types of Microstrip patch antennas in his book “compact and broadband microstrip antennas” New York: J.Wiley and sons,2002[4]. Das and Das has also cited many of such designs and process where multiband operations can be achieved [1]. Hala Elsadek, Member, IEEE, and Dalia M. Nashaat has discussed a V shaped patch antenna which gives multiband and UWB operation at the same time.[5].Dr. Ramesh Garg has discussed many theoretical aspects of bandwidth increment and multi frequency operations in circular patch antenna along with simulations[2].

The proposed antenna in this paper is designed using Ansoft HFSS 14 which works on the Finite Element Method. First the antenna is analyzed using cavity model then by using this software a model is designed to get the desired dual frequency response. The designed antenna resonates at two frequencies 4GHz and 5.8 GHz which are the Receiving and Transmitting Frequencies of standard C band respectively[7]

## II. ANTENNA CONFIGURATION

The geometry of the proposed antenna is as shown in Fig.1. Here Two semicircular slots were cut on the radiating circular patch. Then 4 tuning arms are added to achieve better frequency matching and a good agreement between the S[11] and Bandwidth of the antenna.

The resonant frequency of excitation can be given as [3]

$$f_r = \frac{x'_{nm} \times c}{2\pi a \sqrt{\epsilon_r}} \dots\dots\dots(1)$$

for a physical radius = *a*. After considering the fringing extension modified resonance frequency becomes

$$f_{rTM_{nm0}} = \frac{x'_{nm} \times c}{2\pi a_{eff} \sqrt{\epsilon_r}} \dots\dots\dots(2)$$

where m=0,1,2,3,.....number of half cycle variation along  $\phi$ , and n=1,2,3,..... number of half cycle variation along  $\rho$ . Here the fringing effect is taken into account by using an effective radius [3]

$$a_{eff} = a \left[ 1 + \frac{2h}{\pi a \epsilon_r} \left\{ \ln\left(\frac{\pi a}{2h}\right) + 1.7726 \right\} \right]^{0.5} \dots\dots(3)$$

Here in the proposed antenna the circular patch radius is 19.4 mm. FR<sub>4</sub> epoxy is the dielectric material used here with dielectric constant  $\epsilon_r = 4.4$ . and the substrate height (h) is 1.6 mm Here, *L<sub>p</sub>* and *W<sub>p</sub>* are the length and width of the connecting rectangular slot which gives the patch a phi shape. The values are *L<sub>p</sub>*= 30.8 mm and *W<sub>p</sub>* = 5mm . A , B , C , D are the tuning arms which were added to the patch to obtain best matching and agreement between return loss and Bandwidth. The all over with of the circular ring is 5 mm. The dimension of tuning arm A is

# Face Detection based approach to combat with COVID-19

Suparna Biswas, Senjuti Mazumdar, Sangeeta Rana, S.B. Amreen Saba, Palasri Dhar,  
Sayan Roy Chaudhuri

Electronics and Communication department, Guru Nanak Institute of Technology, Sodepur,  
Kolkata, India, Email: suparna.biswas@gnit.ac.in

**Abstract.** - The global problem at the moment is COVID-19 caused by corona-virus which led to the worldwide lockdown. However there are still people who are not taking proper precautions and maintaining social-distancing while going out for emergency situations. To ensure this the government is trying to monitor the actions of each and every citizen. It is not realistically possible to monitor the actions of each and every citizen. This problem can be possibly solved by the use of machine learning. In this paper we have presented face detection based technique to combat with COVID-19. At first this technique captures the image and detects the face using Viola Jones method. Then the detected face images are classified to detect the mask. It actually detects whether every person have used mask or not. If there present anyone without mask then the system starts alarm to inform it to the responsible authority and to alert the public. Here Principal Component Analysis (PCA) has been used to extract the feature from the detected face images and for the detection of mask K-Nearest Neighbor (KNN) classifier has been used.

**Keywords** - COVID-19, Face detection, Classification, Mask detection.

## 1. Introduction

The name "Coronavirus" comes from the crown like projections on their surface. The meaning of this latin word "Corona" is "halo" or "crown". Coronaviruses are a group of related viruses that causes diseases in mammals and birds. In human coronaviruses cause respiratory tract infections that can be mild, such as common cold. This corona virus is responsible for millions of infections occurring daily and causing thousands of deaths. The virus is spread through direct contact with respiratory droplets of an infected person by coughing, sneezing and touching surfaces contaminating with the virus. Corona virus symptoms are very similar as common cold such as: fever, cough, sore throat, muscle pain, fatigue, and shortness of breath.

## NECESSARY PRECAUTIONS TO BE TAKEN TO AVOID THE RISK OF COVID-19:

- Wear a mask while going outdoor.



Content from this work may be used under the terms of the [Creative Commons Attribution 3.0 license](https://creativecommons.org/licenses/by/3.0/). Any further distribution of this work must maintain attribution to the author(s) and the title of the work, journal citation and DOI.

# GPS Tracking, QR code Scanner Based Application to Help the Health Workers and Common Citizens during Covid-19

Suparna Biswas, Wriju Banerjee, Sanchari Saha, Saswata Sundar Maity,  
Tathagata Bhattacharyya and Subhrajyoti Saha

Electronics and Communication department, Guru Nanak Institute of Technology, Sodepur,  
Kolkata, India, Email: suparna.biswas@gnit.ac.in

**Abstract.** - At the end of 2019, a novel Corona Virus surfaced as a pathogen and eventually resulted in a pandemic situation. The infection rate unleashed havoc worldwide firstly affecting European nations then the US. So, in this paper we proposed a software application which intakes user data to calculate the threat based on the merits of reconstructed survey which prompts the user to check if they are undergoing any of the medically proven symptoms and sends it to the local municipal clinic. This in turn will minimize the need for medical workers to visit door to door constantly at risk of getting infected. This software is equipped with features like GPS tracking, threat level predictor, contamination graph it also determines medicinal urgency etc. Basically, our system is supposed to assist the day to day workers and visit places in scenarios of maximum urgency. This proposed system is used to prevent allowing likely symptomatic as well as asymptomatic users to enter in the hotspot regions' public places such as malls and markets. The application will generate a unique QR code for respective users which will depict their merit based on mandatory survey that whether that person is affected or not. The QR code can be used in order enter the public area places where scanners are placed.

**Keywords** - GPS tracking system, QR code, Contamination graph.

## 1. Introduction

Now days the whole world is suffering from a disease, which is known as Coronavirus disease (COVID-19). The world health organization (WHO) declared the coronavirus disease a pandemic which means it is occurring over a wide area and affecting a high portion of the population. The common symptoms of corona virus are fever, cough, fatigue, shortness of breath but in some of the cases result in mild symptoms like multi-organ failure, septic shock and blood clots. Primarily the



Content from this work may be used under the terms of the [Creative Commons Attribution 3.0 license](https://creativecommons.org/licenses/by/3.0/). Any further distribution of this work must maintain attribution to the author(s) and the title of the work, journal citation and DOI.



# An efficient face recognition method using contourlet and curvelet transform

Suparna Biswas<sup>a,\*</sup>, Jaya Sil<sup>a</sup><sup>a</sup> Dept. of Computer Science & Technology, Indian Institute of Engineering Science and Technology, Shibpur, P.O. Bidanil Garden, Howrah-711 005, India

## ARTICLE INFO

### Article history:

Received 20 March 2017

Revised 09 October 2017

Accepted 29 October 2017

Available online 8 November 2017

### Keywords:

Contourlet transform

Curvelet transform

Classification

Face recognition

Dimensionality reduction

## ABSTRACT

In this paper we propose a novel method for face recognition using contourlet transform (CNT) and curvelet transform (CLT) which improves rate of face recognition under different challenges. We obtain smooth contour information along different directions by applying CNT on the face image while CLT having multiscala, multidirectional and anisotropic properties has been employed to represent the edges more prominently. Pre-processed training images are decomposed up to fourth level using CNT and coefficients of directional subbands are analyzed to obtain the features from the images. In another approach CLT has been applied on the pre-processed face images and considering scale of four and angle eight, different statistical features are extracted from the detail subbands. Finally, we integrate the features obtained from two approaches. High dimensionality of feature space has been reduced by selecting important features depending on the entropy of the transform coefficients. Selected features are applied to recognize the face images using support vector machine (SVM) classifier. Experimental results show that the proposed feature extraction method improves recognition accuracy compared to other methods and efficiently handle the effect of Gaussian noise at levels of 10%, 20% and 30% on Labeled Faces in the Wild (LFW), ORL and FERET database.

© 2017 The Authors. Production and hosting by Elsevier B.V. on behalf of King Saud University. This is an open access article under the CC BY-NC-ND license (<http://creativecommons.org/licenses/by-nc-nd/4.0/>).

## 1. Introduction

In recent years biometric based techniques have been emerged as the most promising option for recognizing individuals. Face recognition offers certain advantages over other biometric methods, such as fingerprints, iris, retina and hand geometry, mainly for two reasons. Firstly the facial images can easily be acquired from a distance and secondly, face images can be collected without any prior knowledge.

Face recognition is challenging in the field of pattern recognition and computer vision for dealing with the images having pose variation, illumination differences and different expressions. Efficient recognition algorithms with appropriate image pre-processing

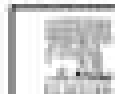
methods may aide to reduce the effect of noise, pose variations and illumination differences in the images. An automatic face recognition method consists of two steps: (i) feature extraction and (ii) design of classifier. However, classification outcome largely depends on the facial feature extraction methods.

Different methods both in spatial and frequency domains have been developed to extracting the features from the face images for person recognition. Recently to analyze the high dimensional signals a theory has been proposed named as multiscale geometric analysis (MGA). Different MGA tools like curvelet (CLT) [Starck et al., 2002; Maudal et al., 2007], bandlet and contourlet (CNT) [Xu and Zhang, 2008; Yu et al., 2005] are proposed for feature generation and data compression as well. N.G.Chitalya and A.Trivedi describe contourlet and Principal Component Analysis (PCA) based method [Chitalya and Trivedi, 2010] for feature extraction and dimensionality reduction in face recognition. They show that the proposed method performs better than the wavelet transforms. Wang et al. [2008] develop an efficient face recognition method based on CNT and SVM. Huang et al. [2010] build a face recognition method based on Haarwavelet invariant features in CNT domain and the results they obtained are effective and competitive with respect to other methods. In Chitalya and Trivedi [2010], author propose an efficient face recognition technique by combining CLT for feature extraction and PCA for dimension reduction. Here

\* Corresponding author.

E-mail addresses: [suparna\\_sil@iitkgsi.ac.in](mailto:suparna_sil@iitkgsi.ac.in) (Suparna Biswas), [jaya@iitkgsi.ac.in](mailto:jaya@iitkgsi.ac.in) (J. Sil).<sup>a</sup> Faculty, Bengal Engineering and Science University, Shibpur P.O. Bidanil Garden, Howrah-711 005, India.

Peer review under responsibility of King Saud University.



Production and hosting by Elsevier

## 1 Sensor materials

2 Performance Improvement of n-ZnO/p-rGO Heterojunction Based Room  
3 Temperature Hydrogen Gas Sensor4 Swapan Das<sup>1</sup>, Sunipa Roy<sup>2</sup> , and Chandan Kumar Sarkar<sup>1\*</sup>5 <sup>1</sup>IC Design and Fabrication Centre, Department of Electronics and Telecommunication Engineering, Jadavpur University, Kolkata  
6 700054, India7 <sup>2</sup>Department of Electronics and Communication Engineering, Guru Nanak Institute of Technology, Kolkata 700114, India

8 \*Senior Member, IEEE

9 Manuscript received February 2, 2021; revised March 8, 2021 and March 21, 2021; accepted April 4, 2021. Date of publication; date of current version.

10 Abstract—This letter reports a room-temperature hydrogen gas sensor based on the nanohybrid structure of ZnO  
11 nanorods (NRs) and reduced graphene oxide (rGO) with better sensitivity. In this nanohybrid structure, ZnO NRs were  
12 grown up by the chemical bath deposition technique followed by the electrochemical exfoliation of rGO layer. The  
13 collaborative hybridization of these two dissimilar sensing elements revealed much better response at room temperature,  
14 which could hardly be achieved by the individual ones. The sensing was carried out at room temperature at ~40%  
15 RH, with hydrogen as a target gas with fastest response and recovery times (17.02 and 27.06 s), which have not been  
16 achieved earlier. The physics behind it is the high carrier mobility of rGO. A very high response magnitude (586.93% at  
17 100 ppm) was found due to the increased number of gas-interaction sites and availability of free surface energy provided  
18 by ZnO NRs and rGO. A comparative discussion elucidating the role of ZnO NRs-rGO junctions has also been presented  
19 correlating the experimental findings.

Index Terms—Sensor materials, heterojunction, high sensitivity, hydrogen, n-ZnO nanorods (NRs)/p-rGO, room temperature.

## 20 I. INTRODUCTION

21 Nanoscale metal oxides have left their impression for improving the  
22 gas sensing performance. C-axis oriented nanostructures like nanorods  
23 (NRs), nanotubes offer several advantages due to their governed 1-  
24 D electron transport kinetics and larger free surface energy [1]–[3].  
25 Realizing a room temperature gas sensor with a substantially high  
26 response magnitude (RM) is quite difficult to achieve due to its slow  
27 adsorption-desorption kinetics.

28 Recently, graphene-based gas sensors showed very high electrical  
29 conductivity and very low response time. Still, pristine graphene is not  
30 a suitable candidate for room temperature sensing [4] possibly due to  
31 low resistivity and low defect density.

32 To overcome the above-mentioned bottleneck, graphene and its  
33 derivative reduced graphene oxide (rGO) paved a new way in the  
34 area of next-generation gas sensors. Hybridization of rGO like ZnO  
35 NRs-rGO is an established nanohybrid in the gas sensor family [5],  
36 [6]. Presence of rGO between adjacent ZnO NRs contributes an  
37 uninterrupted trail for carrier transport from multiple gas-interaction  
38 sites by forming the heterojunction (n-ZnO/p-rGO) among them. The  
39 electrostatic field generated at the space charge region is responsible  
40 for the reduction of activation energy in gas sensor [7].

41 This letter reports a simple approach of fabricating ZnO NRs-rGO  
42 nanohybrid where ZnO was deposited by chemical bath deposition  
43 method and sol-gel [8], [9]. rGO was prepared by an easy electrochem-  
44 ical exfoliation method [10], [11]. The uniqueness of this work lies on  
45 low annealing temperature (100 °C) of rGO, which could not damage  
46 the underlying chemical components of ZnO layer contributing to the  
47 p- and n-type conductivity of the subsequent layer.

After integrating n-ZnO with p-rGO, the device was tested for 48  
hydrogen (100–10 000 ppm) and offered highest RM (RM = 586.93%) 49  
with the faster response (~17.02 s) and recovery time (~27.06 s) 50  
at 100 ppm H<sub>2</sub>. Earlier relevant works with all details have been 51  
represented in Table 1. 52

## 53 II. DEVICE FABRICATION

ZnO seed layers were deposited using standard sol-gel spin coating 54  
by reacting with zinc acetate dihydrate ((Merck, 99.9%), 2.74 gm) and 55  
2 propanol (2-ME, 99.8%) (50 ml). After mixing 1.5 ml diethylamine 56  
as a stabilizer was also added drop by drop to get a crystal clear solution 57  
followed by 24 h aging. The samples (5 mm x 5 mm) were spin coated 58  
(2500 r/min) for 20 s on SiO<sub>2</sub> coated silicon substrate and annealed at 59  
500 °C for 1 h, where ZnO NRs were synthesized by preparing a 50 ml 60  
solution of zinc acetate dihydrate and HMT [hexamethylenetetramine 61  
[(CH<sub>2</sub>)<sub>6</sub>N<sub>4</sub>, Alfa Aesar, Germany]] in deionized water (resistivity 62  
~18.2 M<sub>Ω</sub>-cm) with the ratio of 1:3 [8], [9]. The sol-gel coated 63  
substrate was then immersed horizontally into the solution and kept in 64  
a baking oven for 1 h at 100 °C followed by drying. 65

rGO was prepared by organic liquid-assisted electrochemical exfoli- 66  
ation technique, the details of which have been published in our earlier 67  
publication [10], [11]. Produced rGO nanosheets are dissolved in a 68  
polar aprotic solvent (1mg/ml) dimethylformamide and 10 μL droplet 69  
solution of dissolved rGO nanosheets were drop-casted over the ZnO 70  
NRs using micropipette technique. Total four samples were prepared 71  
and annealed at 100 °C for 1 h. Pd-Ag (70%) contact electrodes were 72  
deposited by e-beam evaporation technique, and fine copper wires were 73  
used to take out the contact. 74

Sensing characteristics of the device toward H<sub>2</sub> were investigated 75  
in a gas sensing system with 40% RH, identical to the one described in 76  
[11]. RM was calculated using the relationship shown in the following 77

Corresponding author: Sunipa Roy (e-mail: [sunipa\\_4@yahoo.co.in](mailto:sunipa_4@yahoo.co.in)).

Associate Editor: J. Gardner. (Swapan Das, Sunipa Roy, and Chandan Kumar Sarkar contributed equally to this work.)

Digital Object Identifier 10.1109/LENS.2021.3072424